



Universiteit  
Leiden

The Netherlands

## Probing single chaperone substrates

Wruck, F.; Avellaneda, M.J.; Naqvi, M.M.; Koers, E.J.; Till, K.; Gross, L.; ... ; He, L.

### Citation

Wruck, F., Avellaneda, M. J., Naqvi, M. M., Koers, E. J., Till, K., Gross, L., ... Tans, S. J. (2023). Probing single chaperone substrates. In S. Hiller, M. Liu, & L. He (Eds.), *New Developments in NMR* (pp. 278-318). Royal Society of Chemistry.  
doi:10.1039/BK9781839165986-00278

Version: Publisher's Version

License: [Licensed under Article 25fa Copyright Act/Law \(Amendment Taverne\)](#)

Downloaded from: <https://hdl.handle.net/1887/3714173>

**Note:** To cite this publication please use the final published version (if applicable).

## CHAPTER 11

# *Probing Single Chaperone Substrates*

F. WRUCK,<sup>a,b</sup> M. J. AVELLANEDA,<sup>a,c</sup> M. M. NAQVI,<sup>a,d</sup>  
E. J. KOERS,<sup>a,e</sup> K. TILL,<sup>a</sup> L. GROSS,<sup>a</sup> F. MOAYED,<sup>a</sup> A. ROLAND,<sup>a</sup>  
L. W. H. J. HELING,<sup>f,g</sup> A. MASHAGHI,<sup>f,g</sup> AND S. J. TANS<sup>\*a,h</sup>

<sup>a</sup> AMOLF, Science Park 104, 1098 XG Amsterdam, The Netherlands;

<sup>b</sup> LUMICKS BV, Amsterdam, The Netherlands; <sup>c</sup> Institute of Science and Technology Austria, Am Campus 1, Klosterneuburg 3400, Austria;

<sup>d</sup> Department of Pharmacology, University of Cambridge, CB2 1PD

Cambridge, UK; <sup>e</sup> Centre of Membrane Proteins and Receptors (COMPARE), University of Birmingham and University of Nottingham, Midlands, UK;

<sup>f</sup> Medical Systems Biophysics and Bioengineering, Leiden Academic Centre for Drug Research, Faculty of Science, Leiden University, 2333CC, Leiden, The Netherlands; <sup>g</sup> Centre for Interdisciplinary Genome Research, Faculty of Science, Leiden University, Einsteinweg 55, 2333CC Leiden, The Netherlands;

<sup>h</sup> Bionanoscience Department of Delft University of Technology and Kavli Institute of Nanoscience Delft, 2629HZ Delft, The Netherlands

\*Email: S.Tans@amolf.nl

## 11.1 Introduction

Elucidating how cells control the conformational state of their proteins is one of the major problems in biology.<sup>1,2</sup> Indeed, most non-infectious diseases are thought to be rooted in the formation of erroneous protein structures, a process exacerbated by cellular stress, ageing, and environmental and genetic factors.<sup>3</sup> It has been well established that molecular chaperones are key to efficient protein folding.<sup>4,5</sup> Important progress has

---

New Developments in NMR No. 29

Biophysics of Molecular Chaperones: Function, Mechanisms and Client Protein Interactions  
Edited by Sebastian Hiller, Maili Liu and Lichun He

© The Royal Society of Chemistry 2024

Published by the Royal Society of Chemistry, [www.rsc.org](http://www.rsc.org)

also been achieved in determining chaperone structures, as well as their conformational changes, biochemistry, and interactions with co-factors. However, we know far less about the underlying molecular mechanisms at the level of substrate conformational changes.<sup>6–8</sup> Yet, during their lifetime, amino acid chains undergo highly diverse conformational transitions that are decisive to success and failure: they can collapse into compact yet dynamic states,<sup>9</sup> fold progressively during their synthesis,<sup>10</sup> become partially unfolded to enable signaling pathways,<sup>11</sup> and get incorporated into protein complexes,<sup>12</sup> protein aggregates,<sup>13</sup> and stress granules,<sup>14</sup> while also being removed from these higher-order structures.<sup>15,16</sup> Though many of these processes have been investigated extensively, it has been difficult to study protein conformation changes directly.

This lack of progress is understandable. Conformational changes of fully folded proteins, such as those associated with allosteric transitions, typically involve a few key states that can be controlled externally and hence can be studied using averaging structural methods such as cryo-EM and crystallography.<sup>17</sup> Conversely, structural states of unfolded and partially folded protein substrates are typified by large conformational ensembles, dynamics from microseconds to minutes, and heterogeneous interactions with chaperones and their ATP-driven cycles.<sup>18,19</sup> These factors pose major experimental detection challenges. In recent years, however, crucial technical advances have emerged that promise to address them more directly. Structural approaches including cryo-EM, NMR, and hydrogen exchange mass spectrometry can increasingly resolve marginally stable complexes, interaction sites and surfaces, and rapid movements within polypeptide backbones, while single-molecule FRET has been pivotal in identifying structural heterogeneity, among many more effects crucial to understanding how protein conformations are affected by chaperones.<sup>8,20–24</sup>

This chapter aims to describe recent advances in probing chaperone function using single-molecule manipulation methods including atomic force microscopy (AFM), magnetic tweezers, and optical tweezers, noting that most studies employed the latter (see Figure 11.1). We thus focus on the substrate rather than the chaperone dynamics and on mechanical probing approaches rather than fluorescence-based techniques. Since its inception, single-molecule manipulation has been pivotal in revealing many important phenomena, ranging from RNA polymerase translocation dynamics to kinesin stepping and multi-step protein folding pathways.<sup>25–28</sup> What this approach lacks in direct structural information, it makes up for in real-time quantification of movements and stability. In recent years, it has been increasingly applied to elucidating protein state control. This first view on the conformational transitions of chaperone substrates has revealed many unexpected effects, ranging from the stabilization of folding intermediates<sup>29–31</sup> to the promotion of folding under tension,<sup>32</sup> the strengthening of polypeptide collapse,<sup>33</sup> and the forceful translocation of looped polypeptides.<sup>34</sup> Hence, now is a good moment to take stock of this new direction and assess how it is altering our understanding of chaperone function and protein state control.

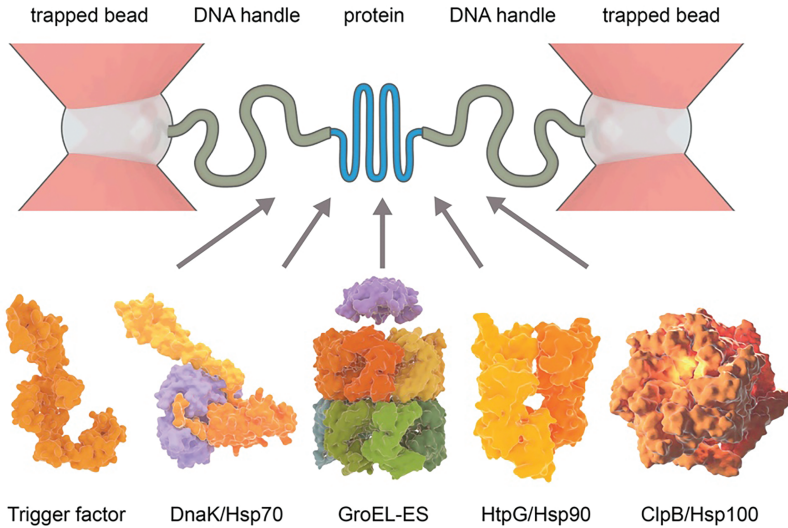


**Figure 11.1** The substrate manipulation approach to studying chaperone function. Protein substrates are held in place by tethering them to DNA handles, which in turn are attached to micron-sized beads that are trapped in focused laser beams. By moving the laser beams, one can mechanically perturb the tethered protein while monitoring its dimensions and internal tension or force in time. In turn, this allows direct probing of diverse phenomena, and how they are induced or altered by chaperones that are free in solution, including unfolding and refolding transitions, intermediate folded states, and their mechanical stability, and gradual collapse processes and refolding probabilities. The use of tandem-repeat protein constructs allows the study of aggregation between them. This approach is increasingly combined with single-molecule fluorescence detection, which can for instance report on the binding and unbinding of single chaperone molecules.

The outline of this chapter will be as follows: after providing background on the optical tweezers technique, we follow proteins from their initial synthesis by ribosomes, to the interactions with the major *E. coli* chaperones including trigger factor, DnaK, HtpG, and GroEL-ES, and then turn to aggregation prevention by the small heat shock proteins and disaggregation by ClpB (see Figure 11.1), and conclude with an outlook where we discuss new challenges and questions for the coming years.

## 11.2 The Optical Tweezers Approach

Optical tweezers have found many applications in physics and the life sciences<sup>35–37</sup> ever since Arthur Ashkin's first description of optical trapping of dielectric particles in liquid.<sup>38</sup> Using near-infrared lasers to form gradient force traps made it possible to indirectly apply pN-scale forces on large molecules, nm-sized motor enzymes and ribozymes (*e.g.* ribosomes), internal parts of cells, and whole living cells in their native environment

without causing optical damage.<sup>39,40</sup> The use of optical traps in single-molecule biophysics has greatly enhanced our understanding of a wide range of molecular motors found within the cell.<sup>41</sup> Optical trap force spectroscopy has enabled researchers to carry out precise measurements of the minuscule forces and displacements that govern many biological processes at the single molecule level.<sup>42</sup>

A simple optical trap is formed by focusing a Gaussian beam to create a diffraction-limited spot using a lens with a high numerical aperture such as an inverted microscope objective.<sup>36</sup> Optical trapping of micron-sized dielectric particles near the focal point of such a gradient trap is easiest explained in terms of conservation of momentum.<sup>43</sup> As light impinges on a transparent spherical particle with a higher refractive index than the surrounding medium, some of the light is scattered, but most of the light passes through the sphere. As illustrated in Figure 11.2a, the combined momentum flux change of the Gaussian beam passing through the sphere results in an overall force experienced by the bead pointing towards the region with the greatest light

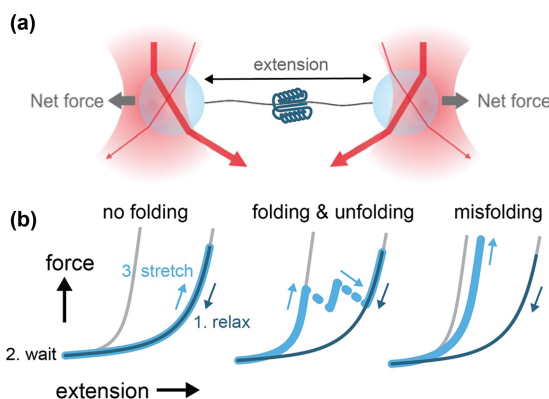


**Figure 11.2** The principle of optical trapping and the protein force spectroscopy approach. (a) Simplified ray diagram depicting the net force experienced by two tethered beads in two optical traps due to refraction of the trapping laser at the surface of the beads (red arrows). Key measured quantities are the extension or distance between the beads, and the net force acting on the molecular construct bridging the two beads. (b) Schematic of resulting force spectroscopy data for a slow folding protein, as it either does not refold (left), does fold and then unfolds again *via* a folding intermediate (middle), or misfolds and then does not unfold during relax-wait-stretch cycles (right). Gray lines indicate the theoretical forces and extensions when stretching or relaxing a compact folded state and an extended unfolded state, using the worm-like chain (WLC) model. Hence, one can detect diverse changes that chaperones can potentially exert. They may change the probability of refolding or induce it against applied forces, promote intermediate folds identified as data following additional WLC curves, but also suppress folded states including misfolds, and alter the stability of intermediate folded states as identified by their unfolding force.

intensity, the center of the focal point. A particle can be trapped near the focal point if this so-called gradient force overcomes the scattering force due to light scattered by the sphere. If unperturbed, the sphere will be trapped at a slight offset along the optical axis from the focal point, where the gradient force balances the scattering force.

Typically, two such optical traps are used in optical tweezers experiments, formed within the focal plane of a single inverted microscope objective, where one trap can be moved or steered relative to the other. Through off-the-shelf surface modifications, one can ‘tether’ individual biomolecules (or biomolecular assemblies) of interest between two such optically trapped beads. By increasing the distance between the tethered optically trapped beads one can stretch the tethered molecule until at some point the trapped beads get pulled out of the center of their traps, imparting a light-momentum change-induced restoring force on the tethered assembly akin to a spring under tension, following Hooke’s law for a narrow range of forces for up to hundreds of pN in force, dependent on the trapping laser intensity as well as the bead size.

Other microscopy techniques can be combined with optical tweezers, such as multi-color confocal microscopy and/or stimulated emission depletion fluorescence microscopy, allowing for correlated force–fluorescence spectroscopy with super resolution.<sup>44,45</sup> Although more difficult to realize, other single-molecule techniques, such as AFM and magnetic tweezers, have also been combined with various fluorescence microscopy techniques, while specific care needs to be taken to enable simultaneous correlated force–fluorescence measurements.<sup>46,47</sup>

Optical tweezers are ideal for exerting pN-level forces on individual molecules or molecular assemblies, while simultaneously detecting length changes on the order of nanometers and force changes as small as 0.1 pN, while filtering out noise due to Brownian motion. Both the spatial and force resolution increase with applied tension. Some custom instruments have even been able to achieve Angstrom-level resolution at high applied forces.<sup>48</sup> This sensitivity enables for instance the detection of conformational changes of individually tethered proteins during folding and unfolding transitions. By tuning the applied forces one can study proteins in partially folded and misfolded states, which is difficult to do by other means (see Figure 11.2b). Single-molecule techniques like optical tweezers have proven essential for the study of protein folding, misfolding, and synthesis,<sup>49–54</sup> which are asynchronous processes that are difficult to observe using ensemble methods. Optical tweezers have been used at the single-molecule level to observe the stepping of motor proteins,<sup>55–58</sup> DNA–protein complexes,<sup>59</sup> the unfolding and refolding of RNA molecules and proteins<sup>60,61</sup> and to provide information on the translation machinery by reporting on the strength of the interaction between the ribosome and mRNA,<sup>62</sup> its translocation along a short hairpin-forming mRNA molecule,<sup>63</sup> as well as the release of an arrested nascent chain.<sup>64</sup> In a similar vein, and of specific interest in this chapter, optical tweezers can provide unique insight into the effects of chaperones

such as trigger factor (TF) and Hsp70 (DnaK) on the folding, misfolding, and aggregation of their substrate proteins.<sup>31,65</sup>

Optical tweezers studies also come with several challenges and considerations. A key initial difficulty is to tether the substrate protein to beads, which is typically done using dsDNA handles (see Figure 11.1). DNA handles and proteins can be attached using cysteine chemistry, enzymatic reactions, and the ligation of long DNA strands to short DNA oligos.<sup>67–72</sup> Performing this step with high enough yields and preserving the native folded state in non-trivial, specifically for proteins exhibiting limited solubility and stability. For attaching the DNA handles to beads one typically employs biotin-streptavidin or DIG-anti-DIG, which can be formed *in situ* within the optical tweezers instrument. One may note that the attached DNA linkers reduce the protein chain entropy, and hence can affect folding in principle. However, this entropy reduction is small compared to the other relevant energies, in particular when folding occurs in the relaxed state at zero tension (see Figure 11.2b, middle). Applied forces effectively tilt the protein's free-energy landscape.<sup>66</sup> This does not affect folding at zero tension, as force is then merely used to probe the folded state after folding (see Figure 11.2b, middle). Landscape tilting does affect quantitative reconstructions of folding energy landscapes of (typically smaller) proteins that fold when under tension. DNA linkers may in principle also interfere sterically, for instance with chaperone binding, as will be discussed more in the GroEL section. High forces can reduce the average tether lifetime and lead to melting of the DNA handles whilst small forces may effectively drown measured displacements in Brownian noise. Hence, most measurements are typically carried out between *ca.* 2 and 60 pN. Depending on the protein substrate of interest, folding pathways may be complex and heterogeneous, in particular when interacting with chaperones. Obtaining data of high quality and quantity is thus challenging and may benefit from automation.

## 11.3 Co-translational Folding

### 11.3.1 Nascent Chains at the Ribosome

In recent years it has become increasingly clear that the ribosome plays an active role in the folding of proteins during synthesis while also facilitating the interaction with other chaperones, such as trigger factors in *E. coli*. Although mostly treated separately, the line drawn between protein synthesis and chaperone action is becoming increasingly blurred. Here single-molecule studies in particular have uncovered some of these intriguing mechanisms. Studying mRNA translation at the single molecule level is challenging, partially due to the highly dynamic nature of the process, but also because of the large number of components and interactions involved. System complexity is a specific challenge in single-molecule investigations, as a malfunction in one component can lead to the failure of the experiment. Indeed, ribosomes are among the most elaborate molecular systems that

have been studied at the single-molecule level. More specifically, the ribosome consists of 2 subunits (termed large and small), which are made up of 3 long rRNA molecules and more than 50 ribosomal proteins in prokaryotes, 4 rRNA, and 79–80 proteins in eukaryotes. This large (*ca.* 20–30 nm) molecular assembly translates mRNA with the aid of aminoacylated tRNAs and several translation initiation, elongation, and release factors. Individual amino acids are linked together within the peptidyl transferase center, from there the newly minted (nascent) polypeptide chain traverses a *ca.* 10 nm long and *ca.* 1–2 nm wide ribosomal tunnel, cutting through the large ribosomal subunit. Emerging at the ribosomal exit vestibule, the polypeptide chain can fold into its native structure. The key enabling factor for single-molecule experiments has been the availability of customizable *in vitro* transcription/translation systems from commercial sources, and the development of specific assays. For nascent chain folding studies, the latter typically involves attaching a (several) kilobase-long DNA handles to one of the ribosomal proteins, and another one to the N-terminus of the stalled nascent chain,<sup>73,74</sup> while active translation can be measured in real time using handles that are attached to the ribosome and the mRNA,<sup>75</sup> the ribosome and the nascent chain<sup>73</sup> or just the mRNA on its own.<sup>63</sup> The experiments usually involve intentional stalling of the ribosome at specific sites and/or the incorporation of artificially labelled amino acids.

Single-molecule studies of translation have yielded crucial insights into this highly dynamic and heterogenous process. For instance, recent single-molecule studies have shown how protein folding can take place during the synthesis of the polypeptide chain.<sup>73,76</sup> This cotranslational folding was shown to be impacted by the close vicinity of the ribosome itself, since the bulk of the ribosome is made up of negatively charged rRNA resulting in electrostatic interactions between the charged amino acids of the nascent polypeptide chain and the rRNA, causing a delay in the folding of the complete newly synthesized protein.<sup>74</sup> Structural studies have shown that some proteins can already form secondary structures and even tertiary structures deep within the ribosomal tunnel.<sup>77,78</sup> In the case of the small zinc finger domain ADR1a a recent single molecule study utilizing optical tweezers and correlated smFRET has demonstrated that folding can in fact be accelerated within the confines of the ribosomal exit tunnel.<sup>79</sup> Strikingly, the tunnel itself is acting like a folding-accelerating chaperone in this case. Such mechanical manipulation experiments allow the nascent chain to be unfolded, while keeping the rest of the system intact, and refolding to be followed in real time upon relaxation of mechanical tension, which is difficult to achieve by traditional refolding experiments that employ chemical denaturants and monitor the mean refolding progress within the population.

The rate of synthesis of proteins is also modulated by the electrostatic interactions between the nascent chain traversing the tunnel and the tunnel (mostly rRNA) itself. Clusters of positively charged amino acids arginine and lysine, and to a lesser extent histidine, can in fact significantly slow down the rate of synthesis.<sup>80,81</sup> The incorporation of multiple prolines in a row can also



lead to temporary stalling of mRNA translation, which can be rescued by proline-specific elongation factors (EFP) in bacteria for instance.<sup>82</sup> Rare codons and mRNA secondary structures also play a role in modulating translation.<sup>83,84</sup> In contrast, forces applied to the nascent polypeptide chain during translation can increase the rate of synthesis by lowering the transition state free energy barrier to peptide bond formation.<sup>85</sup> The simple act of folding on the ribosome exerts a pulling force on the order of up to 10 pN.<sup>86</sup>

The protein synthesis rate plays an important role in cotranslational folding. Slowed and stalled translation gives the N-terminal and already tunnel-traversed segments of the nascent polypeptide valuable time to fold, potentially preventing aggregation with other partially translated proteins within the cytosol in polysomes for instance.<sup>87</sup> The inherent heterogeneity of protein synthesis, where cotranslational folding appears to be tightly coupled to the rate of translation, makes it a difficult system to study using bulk methods. Single-molecule methods such as optical tweezers are increasingly enabling assays that may soon allow us to follow the dynamics and mechanisms of the involved processes in exquisite detail and will help in disentangling the intricate interplay of the many different components and processes involved, especially when it comes to unravelling the cotranslational role of chaperones. See Figure 11.3.

### 11.3.2 Trigger Factor

As soon as they exit the ribosomal tunnel, nascent chains can interact with a plethora of proteins that could affect their folding pathway and dynamics, which optical tweezers can uniquely address. In bacteria, the chaperone trigger factor (TF) is directly associated with the ribosome, at the tunnel exit, and hence it is typically the first chaperone that nascent chains interact with.<sup>88,89</sup> Discovered in 1987,<sup>90</sup> TF is not essential as deletion of the TF encoding gene *tig* seems to be compensated by enhanced action of the chaperones DnaK and GroEL.<sup>89</sup> However, a combined deletion of TF and DnaK was found to be lethal above  $\sim 30^\circ\text{C}$  causing misfolding and aggregation of several hundred cytosolic proteins.<sup>88</sup> Despite sharing a lot of overlapping functions with DnaK and GroEL, the ATP-independent TF appears to engage with protein chains in a unique way, which leaves many open questions about how TF affects the folding process. Over the last decades, many techniques ranging from structural to single-molecule studies have been employed to decipher the function of TF.

The 48 kDa TF protein consists of three domains, the N-terminal, C-terminal, and the PPIase domain, namely because this domain displays catalytic activity as peptidyl-prolyl *cis/trans* isomerase.<sup>89</sup> Together these domains adopt a dragon-shaped structure, where the N-terminal domain forms the “tail”, the PPIase domain the “head” and the C-terminal domain a central body, constituting nearly half of the TF molecule and residing between the N-terminal and PPIase domains with two protruding “arms”.<sup>88</sup> TF binds to the ribosome *via* its N-terminal domain, using the ribosomal exit

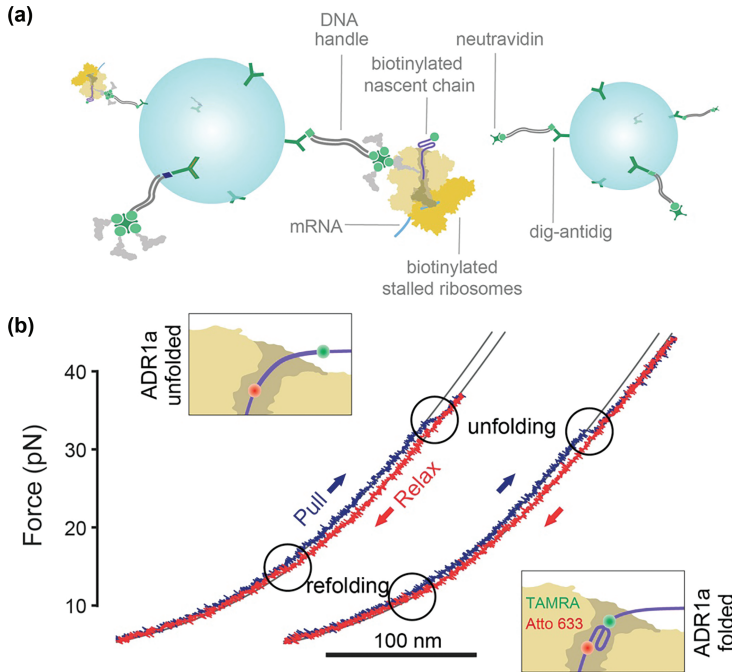


**Figure 11.3** Optical tweezers study of nascent chain folding at the ribosome. (a) Schematic diagram indicating the key components and linking strategy to enable nascent chain manipulation. In the strategy indicated here, biotinylated ribosomes are first linked to beads *via* DNA handles, biotin-neutravidin, and dig-antidig linkages, and then induced to translate a nascent chain, which is biotinylated at the N-terminus and stalled using the SecM strong stalling sequence. After entry into the optical tweezer's apparatus, the final link with a second bead, *via* another DNA handle is made, hence allowing the force spectroscopy approach. (b) Two stretching and relaxation data sets on ADR1a, which is shown to unfold and refold. It showed that refolding is accelerated, when ADR1a was positioned inside the ribosomal tunnel, which is notable given the important steric constraints that the tunnel imposes.<sup>79</sup> By incorporating fluorescent probes into the nascent chain during translocation, simultaneous FRET detection of these unfolding and refolding events was achieved. Data reproduced from ref. 79, <https://doi.org/10.1038/s42003-021-02055-8>, under the terms of the CC BY 4.0 license, <http://creativecommons.org/licenses/by/4.0/>.

site proteins L23 and L29 as major docking site.<sup>91</sup> Ribosome binding stabilizes TF in an open confirmation, creating a cradle-like cavity between the ribosomal surface and the N-terminal tail, and the C-terminal arms of TF, which is about 40 Å deep and 35 Å wide.<sup>92,93</sup> The open cavity is thought to be linked to the function of TF, which is incompletely understood however.<sup>88</sup> For long it has been thought that the open cradle-shaped cavity provides a protective environment for emerging nascent chains, shielding them from

unwanted interactions with their hydrophobic segments as well as with other cellular components, thereby preventing aggregation and protein degradation.<sup>94–96</sup> Thus, TF was believed to fulfill a classic holdase function that stabilizes unfolded states.<sup>97</sup>

However, single-molecule studies revealed several other functions, including the ability to bind and stabilize partially folded states and promote correct folding.<sup>31,98</sup> The first studies focused on fully synthesized protein substrates, away from the ribosome. In cells, TF is present in a two- to three-fold excess relative to ribosomes, suggesting that it may also play a role when not bound to the ribosome.<sup>88</sup> In one study, optical tweezers were used to study the impact of TF on folding pathways.<sup>31</sup> In data from repeated relax-wait-stretch cycles, unfolding and folding transitions are observed as increases and decreases in the extension, respectively, noting that chain segments that are extended by tension can be orders of magnitude longer than folded ones (see Figure 11.2). The maltose-binding protein MBP was found to show a distinctive (un)folding pathway, which was significantly altered in the presence of TF. Partially folded states were “visited” more frequently, for longer, and resisted higher forces, suggesting that TF directly binds the folded part of the protein chain, not just the unfolded chain.<sup>31</sup> At zero force, the protein chain continued to fold, observable by reductions in measured extension, and hence was not irreversibly stabilized by TF. Within tandem-repeated MBP constructs, TF increased the probability of each MBP copy to adopt the native core structure, while decreasing the probability to engage with neighboring MBP copies to form aggregated structures. Together, these data indicated that by binding partially folded structures, TF shields them from non-native interactions with distant sites along the protein sequence<sup>31,94</sup> (see Figure 11.4). Notably, a subsequent magnetic tweezer study showed that the interaction of TF depends on the extension of the substrate chain, as modulated by mechanical tension.<sup>98</sup> Here, the experimental procedure differs slightly, and for instance lets extended and unfolded proteins rapidly jump to a particular force, after which folding is monitored as extension decreases in time. Specifically, for the small globular protein L, it was found that the folding probability for an intermediate force regime (5–9 pN) is increased by up to ~40% in the presence of TF. At zero force the chaperone appeared to hinder the refolding transition, fulfilling potentially a stabilizing function.<sup>98</sup>

Taken together, these single-molecule results provided insights into how TF reshapes the folding free energy landscape (see Figure 11.4). The stabilization of partially folded states indicates the formation of energy minima in between the unfolded and fully folded states, or a deepening of existing ones. Such minima may in fact decelerate folding within individual substrate repeats. But at the same time, the ‘spatial separation’ of different substrate repeats by TF raises kinetic barriers towards aggregated states, as revealed by the tandem MBP repeats.<sup>94</sup> Increased folding rates mediated by TF may also be caused by an overall lowering of the folding energy barrier, which we here refer to as folding acceleration, and hence also

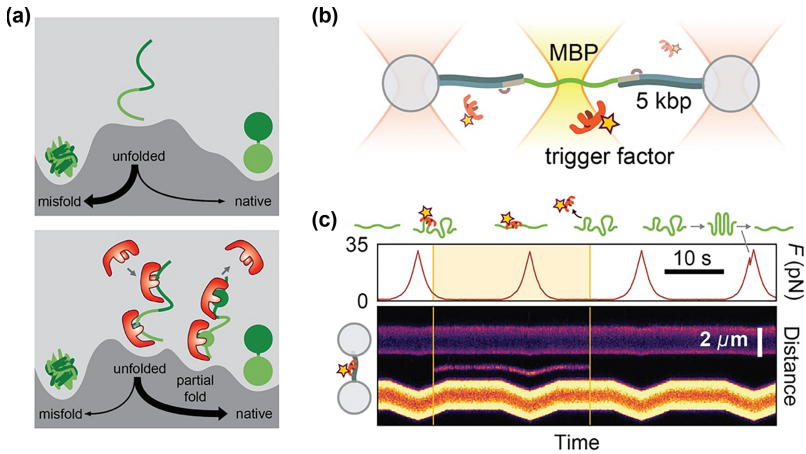


**Figure 11.4** Trigger factor mechanisms revealed by substrate manipulation studies. (a) Cartoon of how folding landscapes can be reshaped by trigger factor, observed by optical tweezers study of single-domain, and engineered multi-domain substrates.<sup>31</sup> Top: Without a chaperone, interactions between domains lead to efficient misfolding. Bottom: Trigger factor binds and stabilizes not only the unfolded chain, but also intermediate states with stable tertiary structure, which corresponds to a formation of energy valleys, or a deepening of existing ones. Owing to the resulting protection against interactions between domains, the folding barrier to misfolds is increased in height, thus limiting misfolding between domains. Hence, native folding is promoted indirectly by limiting misfolding pathways. Trigger factor can also be seen as setting a length scale for native folds, as its binding effectively promotes local over distant intra-chain interactions. Reproduced from ref. 31, with permission from Springer Nature, Copyright 2013. (b) Schematic of combined optical tweezers and fluorescence study of chaperone-substrate interactions. A key technical challenge is to attach long DNA handles efficiently and stably, which is required to increase the distance between the substrate and the bead surface, which is typically highly fluorescent and thus perturbs fluorescence detection at the substrate location.<sup>106</sup> (c) Corresponding kymograph during stretching and relaxation cycles showing a single fluorescently labelled trigger factor binding and unbinding to the tethered MBP protein (thin line in the center).<sup>106</sup> The data are consistent with MBP refolding less frequently when the trigger factor is bound.<sup>31</sup> Here MBP does refold when unbound, as seen by the unfolding feature at the end of the force data in time.<sup>106</sup> Reproduced from ref. 106, <https://doi.org/10.1038/s42004-020-0267-4>, under the terms of the CC BY 4.0 license, <http://creativecommons.org/licenses/by/4.0/>.

impacts single substrates in the absence of aggregation. Folding energy barriers can be effectively reduced by lowering the entropy of the unfolded chain, which may be achieved by multiple contact sites on the chaperone surface, even as contacting must remain dynamic and thus preserve entropy to continue folding, yielding what has been termed a ‘fuzzy complex’.<sup>8,99</sup> The inner surface of the TF cradle exposes hydrophilic and hydrophobic

residues and continuous hydrophobic patches, which may enable TF to interact in this fashion, with substrates of diverse compositions and sizes.<sup>96,100</sup> Stabilization of partially folded states cannot be explained by binding to unfolded substrate segments, however. TF may instead interact with patches on the folded substrate surface, which is exposed when partially folded, and not accessible when fully folded. This idea is supported by the observation that TF does not interact with fully folded substrates in optical tweezers experiments.<sup>31</sup> Additionally, simulations showed that TF employs the flexible arms and polypeptide loop at its tips to interact with its substrates forming “touching” and “hugging” complexes in a dynamic way.<sup>100</sup>

The first single-molecule results on TF roles at the ribosome have been reported recently.<sup>95</sup> A newly synthesized unfolded nascent chain segment of the multidomain protein elongation factor G was found to denature an already synthesized, and folded domain. While the ribosome alone did not protect against this denaturation, TF did, presumably by limiting interactions between the different domains. TF was also found to prevent inter-domain misfolding and as a result speeds up folding, in line with the ‘spatial separation’ model discussed above (see Figure 11.4). The data also showed intermediate states with altered molecular extension in the N-terminal G-domain folding pathway in the presence of TF. Considering the flexibility of TF it was suggested that these altered molecular extensions stem from the binding of the nascent chain to several sites within the TFs inner surface, which would reduce the extension of the protein while keeping it largely unfolded and entropy lowered, thus reducing inter-domain misfolding and promoting domain folding. It was also hypothesized that by forming multiple contacts spaced apart along the client protein chain, entropy is reduced, which in turn may also facilitate subsequent folding.<sup>95</sup>

These novel single-molecule findings thus extend the picture that TF acts as an unfolded chain holdase that decelerates folding. NMR relaxation experiments had indeed shown binding to several distinct regions within TF's inner surface, suggesting TF keeps substrate proteins in an extended, unfolded conformation.<sup>96</sup> Earlier crosslinking studies had indicated that growing nascent chains initially follow a predefined, domain wise, path through the entire interior of TF in an unfolded conformation, which indicated that TF can act as a holdase.<sup>89</sup> Another NMR study even indicated an unfoldase role of TF. By using all its substrate binding sites, TF may be able to unfold transiently formed structures.<sup>92,96</sup> However, since TF cannot use ATP, it is assumed that its unfolding activity is restricted by the intrinsic thermodynamic stability of the substrate.<sup>92</sup> The ability of TF to form dimers has been highly debated.<sup>92,101,102</sup> The dimers may represent inactive storage, as it occludes substrate binding and prevents promiscuous binding of TF.<sup>102–104</sup> TF dimerization potentially could also impose a substrate selection filter, with only high-affinity clients able to bind. Depending on size, folding state, and amino acid composition, the emerging nascent chains increase the affinity of TF for ribosomes by about 2 to 30-fold ( $K_D \sim 40\text{--}700$  nM).<sup>94,103,105</sup>

In conclusion, single-molecule optical tweezer studies have added a new dimension to the bulk-biochemical, NMR, and structural insights, owing to its ability to follow large conformational changes and folding pathway dynamics. Since TF acts in a dynamic reaction cycle governed by translation, with a half-life of TF-ribosome nascent chain complexes of about 15 to 50 s, the detailed dynamics of how TF engages nascent chains are difficult to unveil.<sup>92,94,95,101,102</sup> Optical tweezers combined with fluorescence detection of chaperone binding will be a useful tool to address these questions.

## 11.4 Post-translational Folding

### 11.4.1 The Hsp70 System

The 70 kDa heat shock proteins, termed Hsp70 in mammalian cells and DnaK in bacteria, are a ubiquitous family of chaperone systems that are highly conserved across species and thought to mainly interact post-translationally, though co-translational engagement has been reported in certain cases.<sup>107</sup> They are upregulated in response to temperature and other types of environmental stress, yet also play key roles in normal physiology, as revealed by bulk experimental techniques.<sup>108</sup> Hsp70 chaperones are important to *de novo* folding and many other cellular processes, though the mechanisms of action remain incompletely understood. They aid in the translocation of proteins across membranes, regulate the activity of several key enzymes, and can dis-aggregate certain protein aggregates. Its numerous vital physiological roles are emphasized by the involvement of Hsp70 in many human pathologies ranging from cancer to protein aggregation diseases.<sup>109–111</sup> DnaK is composed of an N-terminal nucleotide-binding domain and a C-terminal substrate-binding domain that contains a moveable 30-amino acid lid. DnaK-peptide binding is regulated by the ATP cycle: when ATP is bound the chaperone exists primarily in its open conformation. Substrate association and dissociation rates are high and affinity is low. Unfolded peptide segments can bind in the substrate binding cleft, which stimulates ATP hydrolysis, in synergy with the co-chaperones (DnaJ and GrpE in *E. coli*). In the resulting ADP-bound state, the lid is predominantly closed. The association and dissociation rates are then significantly lower, resulting in a high affinity.<sup>112,113</sup>

Bulk measurement techniques, however, are less suited to elucidate folding dynamics and intermediate folded states. Such intermediate states typically occur only transiently, in a non-synchronized manner within the population, and cannot readily be stabilized to study them, as for instance is possible with unfolded states using chemical denaturants or temperature. These issues leave key questions at the core of DnaK functioning openly. It has long been thought that DnaK interacts exclusively with unfolded substrate segments. But can DnaK also affect substrates at later stages of folding, as for instance observed for trigger factor in the previous section? Does it mainly protect against aggregation or do more? These questions motivated several force-spectroscopy studies at the single-molecule level.<sup>29,30,114</sup>

However, the involvement of co-chaperones and the ATP hydrolysis cycle posed additional difficulties. The latter is in fact more of a challenge in single-molecule studies, as any binding or conformational event causes heterogeneity in the temporal dynamics at the molecular level, which rapidly become impossible to disentangle, whereas such events are typically averaged out or invisible in bulk assays.

Hence, the single-molecule investigations followed a bottom-up approach, using different model substrates.<sup>29,30,114</sup> One study<sup>30</sup> focused on the maltose binding protein (MBP) constructs also employed in the trigger factor investigation: a single MBP (1MBP) and a tandem-repeat construct (4MBP). In the absence of DnaK, mechanically unfolding 4MBP with optical tweezers and subsequent relaxation to low forces in order to attempt folding, rather yielded misfolding. The latter was seen by subsequent stretching of the construct, which often showed compact structures that either failed to unfold 4MBP (tight misfold) or unfolded in steps larger than expected for one MBP repeat (weak misfold), indicating that small aggregates had formed. Addition of the DnaK chaperone system (DnaK, DnaJ, and GrpE) and ATP buffer showed that the unfolding and relaxation cycles rarely led to tight misfolds, while weak misfolds still formed, and native-like refolding of single MBP repeats increased. These results were consistent with bulk studies, which showed that the DnaK system can promote folding by limiting aggregation.

To probe underlying mechanisms while limiting temporal heterogeneity, DnaK was studied in distinct nucleotide states, in the absence of co-chaperones, acting on the single MBP construct.<sup>30</sup> In the ADP state, unfolded MBP showed a very low refolding rate, consistent with bulk and single-molecule FRET studies,<sup>115</sup> which showed that DnaK-ADP can stabilize unfolded states. More notably, DnaK-ADP was found to also stabilize near native refolded MBP substrates. These compact structures could not be unfolded when stretching up to 65 pN, which is the technical maximum force of the assay (see Figure 11.5a and b). This DnaK-induced stabilization was not observed for fully folded native states of MBP, or for DnaK in the ATP-bound and APO states. Another single-molecule study, which used AFM for the mechanical manipulation of poly-ubiquitin substrates, interestingly also found that DnaK-ADP could stabilize a folding intermediate.<sup>29</sup> Here, the folding intermediate rather appeared to be a molten globule state without a stable tertiary structure. The interactions thus effectively stabilized unfolded conformations, consistent with the MBP study. Consistently, both studies thus revealed that DnaK can bind and stabilize compact substrate conformations (see Figure 11.5c and d), which cannot be explained by the canonical model, and shows that DnaK acts along the folding pathway rather than only at the beginning.

The observed stabilization of folding intermediates raises the question of which part of DnaK is responsible. Truncation of the DnaK lid was found to abolish this stabilization, directly showing its importance in this interaction. Conversely, mutating the groove (DnaK-V426F), which is known to reduce

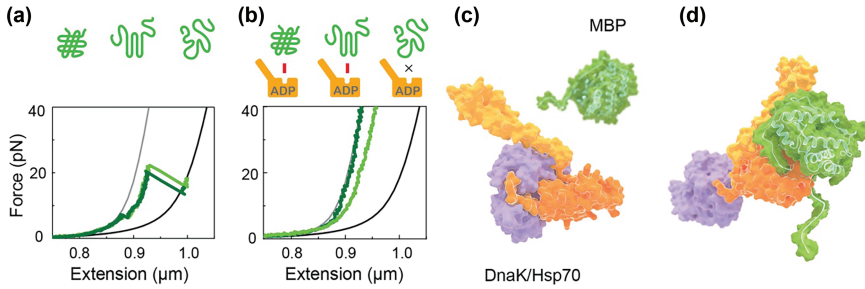


**Figure 11.5** Stabilization of near-native states by DnaK. (a) Typical stretching curves of maltose binding protein after refolding, showing a fully folded state that unfolds, first into a partially folded core state, and subsequently into the fully unfolded state.<sup>30</sup> (b) In the presence of DnaK and ADP, the refolded states can be stabilized, as shown by the lack of unfolding.<sup>30</sup> (c) Structural representation of DnaK in the open conformation and near native MBP. (d) Impression of near-native MBP stabilized by bound DnaK in the ADP state, when it is predominantly in a conformation with the lid domain (yellow) in the closed conformation. Data on DnaK mutants show that both the lid domain and the peptide binding groove in the orange domain play a role in the stabilization.<sup>30</sup> Data reproduced from ref. 30 with permission from Springer Nature, Copyright 2016.

peptide affinity by over 10-fold,<sup>116</sup> did allow for stabilization, though after exposing the substrate for longer periods of time. Moreover, stabilization appeared less strong, as the unfolding forces, while higher than without chaperones, were lower than for *WT* DnaK and occurred *via* folding intermediates. Consistent with this weaker peptide affinity, MBP refolding was re-established, in contrast to *WT* and lid truncated DnaK. Testing the 4MBP substrates indicated that the groove mutant was still able to suppress tight aggregation and aid in limiting the stability of weak misfolds, consistent with the idea that the lid interacts with substrates directly, rather than merely closing the groove. The DnaK lid and groove do act cooperatively, however, as the groove mutation did limit the efficiency of stabilization (see Figure 11.5d). It should also be noted that stabilization against applied force differs from thermodynamic stabilization yet does reveal direct interactions between DnaK and the surface of the near-native folded structure.

DnaJ is another key part of the DnaK system. DnaJ is a dimer of two 40 kDa subunits that can bind and stabilize unfolded proteins, while also interacting directly with DnaK. DnaJ alone was found to suppress MBP and polyubiquitin refolding,<sup>29,30</sup> consistent with its known holdase role. The polyubiquitin study showed that DnaJ recognizes substrates in a force-dependent manner. The measured suppression of substrate refolding became more efficient for larger forces, maximizing at about 160 pN, and then decreased again for higher forces, indicating that DnaJ recognizes a cryptic sequence in extended substrates. One AFM single-molecule study however reported DnaJ rather promoted the refolding of ubiquitin repeats within



poly-ubiquitin constructs.<sup>114</sup> However, DnaJ at the same time limited a misfolding that likely involved interactions between neighboring ubiquitin repeats. Hence, ubiquitin repeats bound by DnaJ may be prevented from aggregating with surrounding repeats, hence allowing the latter to form their native structure. DnaK and DnaJ together were more capable of suppressing misfolding and promoting native folding than either chaperone alone,<sup>29,30,114</sup> consistent with their joint presence *in vivo*. This also means that DnaJ is not dominant in its stabilization of unfolded states, which may indicate that DnaK can promote DnaJ release.<sup>117</sup> However, refolding rates of single ubiquitin and MBP were not shown to be increased by the DnaK system, which could mean that their main role is to prevent aggregation or may also reflect the comparatively high autonomous refolding efficiencies of these specific substrates. The most optimal polyubiquitin refolding was observed for a 1:2 ratio of DnaJ over DnaK.<sup>114</sup>

Overall, the single-molecule investigations have opened a hidden layer of substrate interactions and conformational interplay and produced fundamental extensions of the Hsp70 canonical model. The findings also suggest many new open questions and lines of study. For instance, the structural basis of Hsp70 in complex with folding intermediates remains elusive, which could be addressed by NMR. Hsp70 is also known to be a potent disaggregase, as studied recently.<sup>118</sup> The disaggregation, with the underlying entropic pulling mechanism,<sup>119</sup> and folding promotion roles of Hsp70 appear tenuous, and how they relate remains to be elucidated. Stabilization of folding intermediates by Hsp70 may be important to this issue. Hsp70 could aid disaggregation by competing for sticky patches on the surfaces of incompletely or misfolded substrates, which can become exposed in the dissolution process driven by Brownian motion but also tend to aggregate. Hsp70 could promote folding by transiently capturing and releasing key folding intermediates, driven by ATP hydrolysis, and one can speculate about other mechanisms. More generally, it is unclear whether Hsp70 can lower folding barriers, rather than only raising barriers to aggregated states. These are important open topics for which single-molecule methods are ideally suited. The same holds for elucidating the role of Hsp70 during translation at the ribosome, its dynamic interactions with other chaperones including GroEL, Hsp90, and the disaggregase Hsp100, and its crucial role in many regulatory pathways and cellular malfunction.

#### 11.4.2 GroEL–GroES

Many proteins fail to fold autonomously, with the folding landscape driving them to aggregated, non-native states.<sup>120,121</sup> Chaperones are broadly considered to assist the folding of proteins by shielding them from aggregation interactions.<sup>122</sup> Strikingly, it has remained unresolved whether and how chaperones can also lower folding barriers and accelerate the folding process even in the absence of aggregation. Elucidating this question is difficult. Folding barriers are typically considered kinetic in nature and perhaps also

for that reason poorly understood for proteins of typical sizes. This more direct folding assistance route would also suppress aggregation, by limiting the time spent in unfolded, aggregation-prone states.

The very notion that protein folding can be assisted at all was introduced with the discovery of the barrel-shaped chaperonin complexes,<sup>123</sup> with GroEL/GroES from *Escherichia coli* is the most well-studied example. It is known to confine proteins within its unique cylindrical structure, which provides an environment that is conducive to folding. The GroEL structure consists of two heptameric rings of 14 identical 57 kDa subunits, with a large cavity. GroES is a small ring-shaped oligomer made of seven 10 kDa size subunits, that caps the GroEL cavity in ATP dependent manner.<sup>124</sup> Numerous biochemical<sup>125</sup> and structural studies provided a wealth of information on the GroEL–GroES reaction cycle.<sup>126</sup> Substrates initially bind the hydrophobic apical domains of GroEL and binding of ATP and GroES then release the protein into the cavity where it folds in isolation. ATP binding to the other ring then release GroES and the folded protein from the cavity by intra and inter-rings allosteric signaling.<sup>127</sup> However, the core folding mechanism of GroEL remains debated.<sup>128</sup> A key issue is whether GroEL acts as a passive protein aggregation inhibitor<sup>129</sup> or whether it actively accelerates folding, as discussed above, and if so what mechanism is employed. The notable GroEL closed cavity has suggested that unfolded substrates are sterically confined, which can lower their configurational entropy and hence lower the energy barrier, or alternatively GroEL could promote folding by actively unfolding misfolded conformations.<sup>130,131</sup> Moreover, various questions regarding the functional GroEL–GroES ATP cycles such as the substrate-accepting state of GroEL, the folding competent state, and the precise role of GroES are unanswered.

Recently, optical tweezers were used for the first time to study folding by GroEL–GroES at the single molecule level<sup>132</sup> (see Figure 11.6). Force spectroscopy measurements were performed on wt-MBP and a slow folding dm-MBP variant, in which they were repeatedly unfolded by stretching them at the N- and C-termini, followed by relaxation to zero force to attempt folding during typically 5 seconds, and finally stretching again to assess the new folded state. These experiments indeed showed clear increases in the folding rate with GroEL–GroES present. The effect was particularly strong for dm-MBP, whose core refolding frequency went from less than 10% to about 90% of repeatedly performed relax-wait-stretch cycles. Such an acceleration of folding had thus far not been observed for GroEL or other chaperones and single protein substrates in the absence of aggregation interactions.

To elucidate underlying mechanisms, an approach of freezing the chaperone in its main nucleotide states was used, as was described for DnaK in the previous section. Surprisingly, GroEL in the ADP and ATP-bound states, but without GroES, was also able to accelerate folding, for wt-MBP, dm-MBP as well as for rhodanese protein. The real-time monitoring of optical tweezers proved useful in understanding the underlying mechanism: even before arriving in the relaxed state, the tethered substrate already started to gradually compact as the force was decreasing (see Figure 11.6b). Hence, the

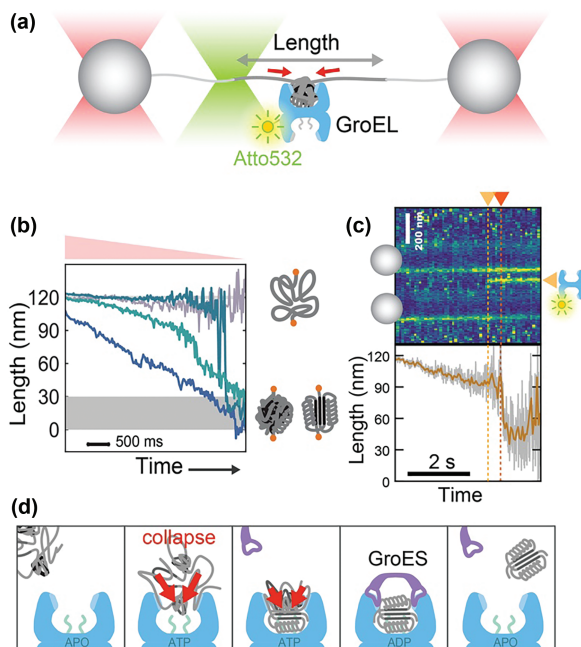


**Figure 11.6** GroEL-mediated acceleration of protein folding by enhancing the collapse.<sup>33</sup> (a) Schematic of joint tweezers-fluorescence setup, which visualizes GroEL binding, while monitoring the length of the tethered protein substrate. Red arrows indicate detected forces that drive the collapse and folding of the substrate within the GroEL cavity. (b) Corresponding contour length in time, showing both gradual and stepwise decreases that indicate collapse and folding triggered by GroEL, for three different dm-MBP molecules with GroEL and ADP. Gray trace: data without GroEL. (c) Kymograph of confocal fluorescence, which scans across the beads and tethered protein. Individual yellow pixels result from freely diffusing GroEL molecules, continuous lines from left to right indicate fluorescence from the bead surface, and the line from the middle to the end, marked by yellow triangles, indicates GroEL binding to the tethered substrate. Corresponding contour length plot of MBP (below) shows the folding step (see red triangle) occurring after GroEL binding (yellow triangle). (d) Model resulting from the optical tweezers data. Unfolded substrates initially bind the apical domains at the GroEL rim, while the unbound substrate segments are drawn into the GroEL cavity by forces that strengthen its general collapse and folding. GroES binding to the apical rim displaces the bound substrate segments, which are then free to collapse and complete folding. ATP drives the substrate and GroES binding and release cycle. Data is reproduced from ref. 33, <https://doi.org/10.1126/sciadv.abl6293>, under the terms of the CC BY 4.0 license, <https://creativecommons.org/licenses/by/4.0/>.

“collapse” of the substrate proteins, which can be discerned without chaperones but in a much weaker fashion, was enhanced by GroEL. Moreover, the stronger the collapse, the higher the subsequent probability of folding.

Control experiments showed that the collapse took place within the GroEL cavity, as truncating the C-terminal tails of GroEL led to decreased collapse and folding. Using fluorescence in combination with tweezers, it could be shown that folding occurred just after a single fluorescently labelled GroEL chaperone bound to the substrate, thus providing direct evidence of accelerated folding of substrates in complexes with GroEL (see Figure 11.6c). In addition, the roles of the apical domains became clearer by using small peptides that bind it competitively, and hence lower substrate affinity. Consistent with acceleration occurring inside the cavity rather than on the apical rim, folding acceleration was still observed. These results were notable given previous work:

First, the tethered nature of the substrates may seem to preclude optical tweezers' manipulation of substrates within a closed GroEL-ES cavity. However, the data showed that hermetic sealing between GroEL and GroES is not required for acceleration within the cavity, and hence that the DNA handles or the protein terminal segments can be sandwiched between GroEL and GroES, consistent with previous observations of polypeptides positioned in between GroEL and GroES.<sup>133</sup> This notion was supported by experiments on a GroEL variant (SR1) that locks GroES in place in a single binding reaction and showed that GroES binding led to apical domain release of the substrate, refolding, and tight stabilization – consistent with the substrate constrained within a closed cavity. In bulk, SR-1 in the ADP state did not show substrate release and folding.<sup>125</sup> This lack of refolding may be due to GroES binding inefficiently to ADP-saturated SR-1 when the substrate is already bound to the apical ring, or that full release of the protein and subsequent folding then fails. Encapsulation can be forced for certain substrates with ADP though without full release and folding.<sup>134</sup> Hence, even though ADP will support GroES binding to GroEL-APO or SR1, if there is substrate protein on the ring first, GroES may not efficiently bind over (large) substrate proteins, or not properly release the protein.

Second, folding acceleration by GroEL alone had not been observed before. Yet, previous work is not inconsistent, as different states and transitions are detected. Specifically, the substrates refolded by GroEL alone were near-native and still complexed with GroEL, shown by increased unfolding forces as for DnaK-ADP in the previous section, rather than fully native and released, which is needed for detection in bulk assays.<sup>24,125,131,135</sup> Indeed, the averaged refolding signal in the latter typically evolves over minutes,<sup>125,135,136</sup> whereas single molecules are observed to fold within seconds of contact. Single-molecule FRET is closer to the optical tweezers data, as it also allows for the detection of sub-populations that follow different pathways. For instance, the ATP and ADP states of GroEL alone consistently showed bimodal distributions of FRET efficiencies for labelled substrates.<sup>136</sup> On the other hand, single-molecule FRET cannot follow GroEL interaction and folding events in time, nor easily distinguish between partially folded and collapsed states, which is key to showing accelerated formation of near-native states.

Third, the observed acceleration mechanism differs fundamentally from previous models (see Figure 11.6d). Enhancing the collapse brings residues together, which must contact to fold, and hence lower folding barriers. At a microscopic level, the hydrophobic effect is thought to drive polypeptide collapse, and it has been shown that it can be altered by nearby surfaces, and it would be of interest to study such water-related phenomena in the context of chaperones.<sup>137–140</sup> Interestingly, substrates in complex with other chaperones including Spy and Skp have also been found in compact and dynamic molten globule states using NMR,<sup>8,141</sup> suggesting that collapse enhancement could be a more general chaperone feature. For GroEL–GroES, various other mechanisms have been proposed. Lin *et al.*<sup>23</sup> observed a compact and expanded intermediate state of Rubisco using ensemble FRET, in line with GroEL promoting folding by unfolding misfolds. Compact intermediates were also observed by Chakraborty *et al.*<sup>131</sup> dm-MBP in bulk assays, as well as eight-fold enhanced folding rates in the presence of GroEL–GroES, explained as GroEL–GroES lowering the folding barrier by reducing the entropy of the unfolded substrate. Other data instead suggested that aggregation suppression by GroEL is central to observed increased dm-MBP refolding,<sup>142</sup> while experiments at very low (100 pM) dm-MBP concentrations that preclude aggregation still showed acceleration.<sup>143</sup> An active folding role of the GroEL cavity was also confirmed by Weaver *et al.*<sup>144</sup> who studied another stringent substrate PepQ, using fluorescence and cryo-electron microscopy. It was also found that the amphiphilic GroEL C-termini tails inside the cavity directly interact with the PepQ folding intermediate deep inside the GroEL cage.<sup>23</sup> Using single-molecule FRET, Hofmann *et al.*<sup>145</sup> reported no change in the folding rates of the N and L regions of rhodanese with and without GroEL–GroES, while the C domain folded two orders slowly in the presence of GroEL–GroES. However, Priya *et al.* reported a higher folding yield of the freeze–thaw rhodanese in the presence of GroEL–GroES, due to the unfolding of the misfolded proteins.<sup>135</sup> These and other folding mechanisms are not mutually exclusive and could act in conjunction.

The dual-barrel nature of GroEL and resulting dual GroES binding sites are also notable structurally. By fluorescently labelling the slow ATP hydrolyzing D398A GroEL variant, Takei *et al.*<sup>146</sup> used single-molecule total internal reflection microscopy to localize GFP proteins at GroEL–GroES sites. The authors demonstrated the formation of symmetric or football complexes<sup>147</sup> and observed the simultaneous folding of two GFP molecules within two GroEL–GroES complexes. The data showed that the football complexes were not short-lived intermediates and were observed in the presence of both denatured and folded substrates. Whereas dual color fluorescence correlation spectroscopy measurements<sup>148</sup> showed that these complexes were appreciably detected only in the presence of unfolded substrates while in the presence of folded or in the absence of proteins they were rarely observed. Noshiro *et al.*<sup>149</sup> used high-speed AFM imaging and also confirmed the formation of symmetric complexes. Interestingly, the authors reported that such complexes are not short-lived intermediates but have

lifetimes ranging from 1.5 to 2.6 seconds and their frequency only moderately depends on the protein conditions.

In summary, single-molecule studies have provided a new view of how polypeptide chains can be impacted by GroEL–GroES. They indicate that true folding catalysts exist, with catalysis being enabled by strengthening the collapse. The ability to monitor substrate conformational changes inside the GroEL cavity opens up the possibility to study other substrates, GroEL–GroES dynamics, the role of GroEL in co-translational folding, as well as the human homolog TRiC/CCT. This optical tweezers approach may also be used to elucidate the role of collapse modulation in protein phase separation and more broadly throughout the protein quality control machinery.

### 11.4.3 Hsp90

Heat shock protein 90 (Hsp90) is a highly conserved ATP-dependent chaperone that is essential in eukaryotic cells. It is a highly abundant protein involved in protein folding that often works in tandem with Hsp70<sup>150</sup> to promote protein folding efficiency.<sup>151</sup> In contrast to Hsp70, Hsp90 serves a narrower clientele which includes 60% of the protein kinases, 30% of ubiquitin ligases, and 7% of transcription factors. Hsp90 often shows important functional interplay with Hsp70 and typically recognizes highly unstable proteins.<sup>152</sup> For example, in a study of FANCA (Fanconi anemia group A) mutants it was shown that mutants that preferably bind Hsp90 over Hsp70 show a less severe phenotype than mutants binding Hsp70.<sup>153</sup> Hsp90 is important for protein homeostasis, for example during heat shock but also plays an important role during cell growth and proliferation<sup>154</sup> which resulted in the development of Hsp90 inhibitors as anticancer agents.<sup>155</sup> Despite these important cellular roles, not much is known about the conformational changes that Hsp90 imparts on its substrates, indicating a need for single-molecule investigations.

Hsp90 consists of three domains – an ATP binding domain, a client and co-chaperone binding domain, and a dimerization domain. The folding of Hsp90 was used as a model for the folding of multi-domain proteins and studied by manipulation with optical tweezers.<sup>156</sup> The study described the folding kinetics of monomeric yeast Hsp90 (Hsp82). They found that the dimerization domain folds in line with the classical two-state model of folding of a small protein. In contrast, the client binding and ATP binding domain show intra- and inter-domain misfolds slowing down the folding of Hsp90 significantly. An optical tweezers study of the same group in 2018 revealed similar folding rates of bacterial Hsp90 (HtpG) and yeast Hsp90, while the ER paralog Grp94 folding is slower and has altered highly stable charged linker which provides a more rigid interface between the ATP binding domain and the client/co-chaperone binding domain. These notable findings on the role of domain interactions during the folding of this important chaperone raise key questions about its function.<sup>157</sup>

Hsp90–client interactions have proven to be notoriously enigmatic, even as recent models provide fresh structural insight. Clients were found to be unstructured for tau,<sup>158</sup> semi-unfolded for Cdk4,<sup>159</sup> or in the near-native folding state for the Glucocorticoid Receptor,<sup>160,161</sup> highlighting different modi operandi of Hsp90. An optical tweezer study of the effect of bacterial and human Hsp90 on clients shines more light on Hsp90 molecular function.<sup>162</sup> In contrast to previous mentioned studies, optical tweezers were used to study how the client conformation is affected, by interactions with Hsp90. Compared to the chaperone–substrate systems discussed in the other sections, a specific challenge here is the typically disordered and structurally heterogeneous nature of the Hsp90 clients. This not only renders the biochemistry of DNA handle and bead attachments far more inefficient and complex, but also introduces the need to consider conformational ensembles rather than the classic chaperone task of achieving distinct folded states. Studies were performed mainly on Luciferase, and its interaction with the bacterial Hsp90 (HtpG), as well as on the wild-type receptor ligand binding domain of the human glucocorticoid receptor, and its interactions with human Hsp90. During the relaxation of mechanically unfolded client chains, it was found that Hsp90 can promote a gradual contraction of the client chain, in an ATP-stimulated manner and despite counteracting forces. Interestingly, the Hsp90-induced gradual contractions are reminiscent of the collapse enhancement seen for GroEL in the previous section, though the dependence on ATP hydrolysis also sets it apart. Polypeptide collapse itself is thought to be key to autonomous protein folding.<sup>163–165</sup> The Hsp90 interactions were also shown to suppress misfolding and aggregation, which typically involve contacts between more distance residues. The experimental findings thus indicate a model where Hsp90 stimulates local intra-chain interactions within unstable clients and suppresses distant ones. Such promotion of local interactions has also been proposed as a mechanism of action for trigger factor<sup>31,100</sup> and DnaK,<sup>30</sup> as discussed in earlier sections of this chapter. In contrast to these chaperone systems, however, the local folds induced by Hsp90 can be significantly smaller (tens or residues or less). Another difference with trigger factor is the reliance of Hsp90 on the ATP hydrolysis cycle,<sup>100</sup> though the precise role of the latter in substrate compaction is still unclear. It also remains an open question what the structural basis is of these Hsp90-induced conformers, how heterogeneous and dynamic they are, and how and where they interact on the Hsp90 surface. The role of these conformational effects at the single-molecule level on the interplay between Hsp90 and Hsp70 is also a major new chapter that remains unresolved.

Probing the dynamics of proteins that are conformationally unstable and heterogeneous, and closer to being disordered, as well as their interactions with the protein quality control machinery, is one of the next challenges for single-molecule protein manipulation. Overcoming the technological hurdles is relevant, given the many interesting and fundamental open questions we have about these protein systems, and their importance in various medical conditions.

## 11.5 Controlling Protein Aggregation

### 11.5.1 Small Heat Shock Proteins

Small Heat shock proteins (sHsps) are a highly diverse family of molecular chaperones. They are characterized by an  $\alpha$ -crystallin domain (ACD) of 90 amino acids, flanked by N- and C-terminal extensions.<sup>166,167</sup> During stress conditions, sHsps are the first line of defense. They co-aggregate with misfolding proteins to prevent the formation of highly stable aggregates.<sup>168,169</sup> When the period of stress has passed, sHsp-associated protein substrates can be re-solubilized and refolded by ATP-dependent disaggregation chaperones Hsp70 and Hsp100.<sup>170,171</sup>

Among the various species of sHsps, manipulation studies of protein substrates at the single-molecule level have been performed on Hsp42, which is one of the two sHsps of yeast.<sup>169</sup> In this study, a construct of four maltose-binding proteins arranged in tandem (4MBP) was unfolded and allowed to refold in the presence and in the absence of Hsp42, using optical tweezers. As shown in the previous sections on trigger factor and DnaK, the 4MBP construct effectively provides high local protein concentration, and can mimic the formation of mini aggregates. Mechanically stretching natively folded 4MBP yields a gradual unfolding transition followed by four distinct unfolding events. The former corresponds to the C-terminal  $\alpha$ -helixes unfolding and detaching from the core MBP structure, and the latter to the unfolding of the four MBP core structures, as characterized by a change in contour length of 92 nm and an unfolding force of 25 pN, on average. In the absence of a chaperone, upon relaxation to low force, the exposed internal segments of different MBP repeats find a chance to interact with each other and form non-native contacts between them. The subsequent stretching pulls show two kinds of aggregated structures: (1) compact structures that withstand forces over the experimental maximum of 65 pN, and are termed “tight aggregates”, and (2) compact structures that do unfold, but then release a chain segment that exceeds the length one MBP core structure, referred to as “weak aggregates”.

In the presence of the Hsp42 chaperone, protein aggregation within the 4MBP construct was found to be partially suppressed. Specifically, the tight aggregates that were abundant in the absence of chaperones were no longer detected, even as weak aggregates were still observed. In addition, a substantial increase in the formation of native-like core structures was detected. The latter is notable, as current models in which sHSPs suppress aggregation by binding and stabilizing non-folded protein segments would rather suppress any tertiary structure formation. To further investigate the nature of these native-like core structures, the authors probed a single maltose binding protein construct (sMBP). The results showed that core structures formed with Hsp42 present are less force-resistant than the native core state, with a mean unfolding force of  $\sim 15$  pN. These data suggest that Hsp42 directly interacts with near-native partially folded



structures of its substrate. Subsequent hydrogen exchange mass spectrometry confirmed the ability of Hsp42 to stabilize near-native substrate states. Through its interactions, Hsp42 could interfere with native intramolecular substrate contacts, and hence prevent conversion to the fully native state, yield a lower resistance to forced unfolding, and limit aggregation by physically separating sequestered protein monomers.<sup>169</sup>

Another chaperone that was observed to bind near-native structures is Hsp33.<sup>172</sup> Like sHsps, Hsp33 is an ATP-independent chaperone that suppresses aggregation. However, it is redox-regulated and undergoes major conformational changes upon exposure to oxidative stress. Active Hsp33 has intrinsically disordered regions that provide a binding site to unfolding substrate proteins.<sup>173</sup> Optical tweezers studies on the same 4MBP construct in the presence of an increasing amount of (active) Hsp33 showed that a significant part of the 4MBP chain now remained unstructured. These data indicated that Hsp33 binds extended polypeptide chains and suppresses both aggregation between MBP repeats and folding transitions within repeats. Interestingly, they also showed significant increases in the relative proportion of MBP cores over aggregates during refolding, which indicated a form of selectivity for native-like structures. To disentangle aggregation and refolding effects, the authors probed sMBP constructs in the presence of Hsp33. It showed a decreased refolding rate, consistent with binding and stabilizing unfolded conformations. The sMBP and 4MBP data could be described using a statistical physics model that systematically defines the ensemble of states of folding and Hsp33 binding that the 4MBP system can be in. It indicated that native folding could be promoted effectively, by limiting the options of unfolded segments to aggregate, rather than promoting folding directly, as for instance observed for GroEL-ES in a previous section of this chapter. In addition, the data also showed that the native-like core-structures were smaller in size than the native core fold. One may speculate that these intermediate states are stabilized by the competitive binding of the intrinsically disordered regions of Hsp33.

A recurring theme hence is that these anti-aggregation chaperones not only bind unfolded, but also near-native conformations, manifested either by reduced stability against forced unfolding or a reduced size of near-native structure. These capabilities allow the chaperones to interact early along the unfolding pathway and could protect them from further unfolding, which may be a more efficient way to limit aggregation but could also accelerate refolding of the native structure once the cellular stress is relieved. The findings raise questions on the elementary differences and similarities within the large family of sHSPs.<sup>174</sup> One may speculate that different HSPs selectively act on certain types of substrates based on the unfolding pathway and early unfolding intermediates of the latter. The ability to probe substrate conformations in a wide range, from unfolded state to partial fold and multi-protein mini aggregates will be a useful tool to dissect their modes of action.

## 11.5.2 The ClpB Disaggregase

Beyond assisting protein folding and preventing protein aggregation, some chaperones have evolved the important ability to rescue and reactivate proteins trapped within aggregates.<sup>13</sup> In metazoans, this task is performed by Hsp70, Hsp110 and a complex network of J-proteins.<sup>175</sup> While their disaggregation mechanism remains largely unknown, recent studies suggest that it relies on entropic pulling.<sup>107,118,176–178</sup> In bacteria, protein disaggregation is mediated by a highly specialized chaperone, ClpB. This donut-shaped protein belongs to the AAA+ class of translocases and consists of an N-domain that binds its substrates, a middle domain that regulates its ATP activity through interaction with DnaK, and a C-terminal domain featuring its catalytic activity.<sup>179</sup> Regulation of ClpB activity is crucial for cell homeostasis, as evidenced by the fatal toxicity of unrepressed mutants,<sup>180</sup> yet the details of the interaction between DnaK and the ClpB middle domain are not fully understood. Recently, single-molecule FRET was used to reveal that the middle domain dynamics were remarkably fast, allowing precise tuning of ClpB activity.<sup>181</sup>

Despite the central role of ClpB in protein homeostasis within bacteria, its underlying mechanism has remained controversial until very recently. The processivity of other structurally related AAA+ translocases, such as ClpX and ClpA, was demonstrated a decade ago using optical tweezers,<sup>182–184</sup> but could not be established for ClpB. In fact, a series of studies using stop-flow suggested that ClpB and its yeast homologous Hsp104 were non-processive and could only translocate a couple of substrate amino acids at a time before disengaging.<sup>185,186</sup> Instead, it was proposed that ClpB could function similarly to the metazoan machinery through entropic pulling or Brownian ratcheting, also consistent with structural studies.<sup>187</sup> Remarkably, bulk studies have also shown that ClpB can process aggregates flanked by stable, folded proteins.<sup>188</sup> The authors suggested that the chaperone can accommodate several polypeptide chains within its central pore simultaneously – despite the lack of supporting structural evidence – and hence process the substrate by threading a polypeptide loop. At the same time, a recent single-molecule AFM study showed that the ring can open and close dynamically,<sup>189</sup> indicating that ClpB can wrap itself around internal segments of polypeptide chains, without the need for open ends. This finding offers an alternative explanation for the bulk data without the need to invoke multiple-chain translocation.

Unambiguous evidence for both processivity and loop extrusion was recently obtained using a combination of optical tweezers and single-particle fluorescence tracking, at a resolution below the diffraction limit.<sup>44</sup> In the study, a substrate protein (maltose binding protein or MBP) tethered between two trapped beads was first unfolded and then relaxed to a low force that prevented refolding. Of note, and in contrast to previous optical tweezers studies on translocases, the substrate did not present any free ends in the chosen configuration. This state can be argued to resemble a

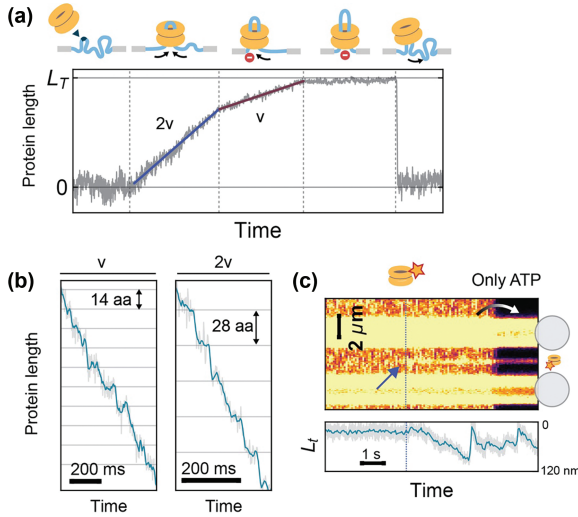


**Figure 11.7** Processive substrate translocation by the disaggregase ClpB. (a) Length of the looped and translocated part of the protein chain, as determined by measured decreases in overall distance between the substrate N- and C-termini.<sup>34</sup> After ClpB binding, the translocated length increases continuously until the entire chain is translocated, showing processive action. The speed halves at a certain moment, consistent with a switch from translocating two arms of the loop to one arm when ClpB encounters the DNA handle on the other arm, until ClpB also encounters the second DNA handle and arrests fully. (b) High-resolution data showing that translocation occurs in steps, with the step size being two-fold smaller when the translocation speed halves.<sup>34</sup> These data are consistent with both arms translocating simultaneously through the central ClpB pore. (c) Fluorescence kymograph showing fluorescent ClpB binding (blue arrow), whose position can be used to determine the translocation of each arm independently<sup>34</sup> (not shown). Medium is switched from with labelled ClpB to without (only ATP) to reduce background.  $L_t$  indicates translocated length. Data is reproduced from ref. 34 with permission from Springer Nature, Copyright 2020.

native ClpB substrate, as the termini of an aggregated protein are more likely to be buried inside the aggregate – thus unavailable, like in the tethered substrate –, while internal segments are exposed on the surface. The addition of ClpB and ATP to the tethered substrate resulted in gradual contractions and sudden releases in the substrate length, indicative of processive protein translocation (see Figure 11.7a).

How can ClpB translocate substrates that do not present free ends? While the chaperone could transiently open in order to engage on an internal polypeptide segment, translocation would then not produce contractions in the used optical tweezers setup (as an analogy, a ring sliding along a string held by both ends would not generate any tension or pulling). To decipher the translocation topology, the authors implemented fluorescence detection

together with force spectroscopy measurements. By imaging the position of a single fluorescently labelled and bound ClpB, one could measure its distance from both termini of the extended substrate – and hence deduce the length of the translocated part of the substrate (see Figure 11.7b). These dynamic data revealed that ClpB can indeed thread a polypeptide loop, like threading a string through the eye of a needle, and proceeds to translocate the loop in a highly processive fashion, without pausing until the end of the MBP substrate. The data also show that two chains can be accommodated in the central pore. Notably, ClpB was seen to switch between translocating either of the two chains or both simultaneously (see Figure 11.7a).

The observed polypeptide loop extrusion may be a universal strategy in protein processing systems, as recent studies suggest handling of multiple substrate chains by other translocases like p97 or Vps4.<sup>190,191</sup> Dissecting the complex dynamics that underlie this process is challenging, and optical tweezers constitute a key tool for this aim. In the ClpB study, measurements at high spatial and temporal resolution showed individual translocation steps.<sup>44</sup> Remarkably, when only one chain was translocated, the step size was 14 residues, and it doubled to 28 residues when two chains were translocated simultaneously (see Figure 11.7b). Given the structural evidence that each ClpB subunit can displace the substrate by 2 aminoacids,<sup>192</sup> the findings suggested a model in which all six ClpB subunits fire one after another in rapid succession (too fast to be resolved as individual steps), followed by a pause, after which a new firing sequence produces another observable step. A recent study used single-molecule FRET to explore the ultrafast dynamics of the pore loops on a ClpB subunit, and the findings pointed to a Brownian-ratchet rather than a hand-over-hand mechanism.<sup>193</sup> Furthermore, given that translocation can take place against remarkably high forces of up to 50 pN,<sup>44</sup> it is a puzzling question how ClpB can maintain such a strong grip on both chains during translocation, while allowing them to slide past each other. Structural studies have shown that nine to ten pore loops inside the ClpB channel – which mediate substrate contact and translocation – are constantly in contact with the substrate (a single polypeptide chain), which explains the tight grip of ClpB on a single chain.<sup>192–194</sup>

How the presence of two chains inside the pore affects chaperone–substrate contact arrangement and coordination remains an important open question. Further structural studies using dedicated substrates (like circular peptides<sup>191</sup> or unfolded polypeptides flanked by stable domains<sup>188</sup>) will be important in elucidating these issues. Optical tweezers experiments using mixtures of monomers with impairing mutations could also shed light on the coordination between the subunits and their interaction with the substrate, as has been shown for other AAA+ translocases.<sup>195–197</sup>

These results provide a more complete picture of the disaggregating mechanism of ClpB. Interestingly, ClpB and its closely related yeast homolog Hsp104 exhibit different disaggregation efficiencies depending on the nature of the aggregates, amyloids in particular.<sup>198</sup> It is still unclear whether

this difference can be solely explained by substrate specificity and recognition (mediated by the N-terminal, which has diverged between both chaperones<sup>199</sup>), or rather the underlying disaggregation mechanism being radically different depending on the topology of the aggregated substrate. Optical tweezers studies of disaggregation using other substrates (such as prion or disordered proteins<sup>200,201</sup>) can provide useful insights, as it is viable to observe the real-time action of ClpB on individual aggregates.<sup>44</sup> Harnessing the disaggregation power of ClpB and Hsp104 to treat human disorders in which uncontrolled protein aggregation seems to be involved (such as Parkinson's or Alzheimer's diseases) is a possibility recently explored,<sup>202</sup> yet much more research is needed to fill the knowledge gaps.

## 11.6 Outlook

In the past decade, optical tweezers and other manipulation methods have begun to contribute a direct view of how cells control protein conformations. Unlike many other methods, the detection principle is essentially independent of the protein state, which has resulted in surprise findings ranging from the promotion of intermediate folds to the modulation of collapse strength, and the processive translocation of polypeptide loops. Hence, a picture emerges of far more diverse conformational steering than previously reported, with chaperones targeting a host of protein states and transitions throughout the folding landscape.

Within this diversity, common features are also emerging. Specifically, most chaperone systems appear to interact not only with unfolded protein chain segments but also with segments exhibiting tertiary structure – and hence also bind protein surfaces rather than extended polypeptides or molten globules only. This feature has been observed for most studied systems, including trigger factor, Dnak/Hsp70, HtpG/Hsp90, GroEL–ES, and the small heat shock proteins, with a notable exception for the secretion pathway chaperone SecB.<sup>203</sup> Such interactions with tertiary structures could allow chaperones to remain associated during folding, protect sticky patches on the surfaces of partially folded states against aggregation, and could potentially also lower folding barriers. Its structural basis also remains an open question. We surmise that these exposed sticky surface patches, which ultimately become buried in the native states, are areas of chaperone contact.<sup>31,204</sup> Another emerging question is whether and how chaperones achieve direct folding acceleration, beyond the indirect promotion of folding *via* aggregation suppression. Folding acceleration was observed for substrates within the ribosomal tunnel and GroEL, which raises the question of whether a cavity, the hydrophobic effect, and the water structure play key roles.<sup>137,139</sup> The involved polypeptide collapse in GroEL offers a notable link to NMR observations of diverse chaperones interacting with molten-globule states.<sup>8</sup> Indeed, collapse modulation could be a more general mechanism to control protein states, including for instance phase-separated states.<sup>205</sup>

The foundational importance of protein states indicates various other urgent questions that are opened by these manifestations of conformational control. Nascent chain folding is one practically uncharted territory. While early models suggested that most chaperones act post-translationally, and hence decreased the relevance of this issue, recent work increasingly indicates ubiquitous co-translational functions for many chaperones.<sup>206</sup> Moreover, the selective ribosomal profiling method that is powerful in revealing them also points to protein–protein assembly as a major co-translational process.<sup>207</sup> Indeed, recent work revealed over 800 proteins in human cells that homo-dimerize during their joint translation, establishing co-translational assembly as a ubiquitous phenomenon.<sup>208</sup> These observations raise crucial questions on the conformational basis, the relation between folding and assembly, and the role of chaperones, which can be uniquely addressed with single-molecule manipulation. On a more basic level, it generally remains unclear how substrate conformational changes are correlated with (co)chaperone binding events and the ATP cycle. It was possible to show how GroEL binds first and folding occurs later. Various alternatives may be exploited, however. Chaperones may stabilize spontaneously formed folded structures, first bind and then actively unfold folded or misfolded states or engage in a temporal interplay with other chaperone systems, as suggested for Hsp70 and Hsp90.<sup>150,209</sup> The access to substrate conformational changes and real-time detection of (co)chaperone binding and unbinding will be important to disentangle these critical interdependencies.

Addressing these and many other questions will be an intriguing challenge for the coming decade. It also invites a deeper integration of different techniques, with the aim to connect insights at the structural, dynamic, and cellular levels. Doing so has the potential to overcome the inherent limitations of different approaches, and to reveal yet-unknown manifestations of protein control within cells.

## References

1. J. Tyedmers, A. Mogk and B. Bukau, Cellular strategies for controlling protein aggregation, *Nat. Rev. Mol. Cell Biol.*, 2010, **11**, 777–788.
2. D. Balchin, M. Hayer-Hartl and F. U. Hartl, In vivo aspects of protein folding and quality control, *Science*, 2016, **353**, 13.
3. J. S. Valastyan and S. Lindquist, Mechanisms of protein-folding diseases at a glance, *Dis. Models Mech.*, 2014, **7**, 9–14.
4. Y. E. Kim, M. S. Hipp, A. Bracher, M. Hayer-Hartl and F. U. Hartl, Molecular chaperone functions in protein folding and proteostasis, *Annu. Rev. Biochem.*, 2013, **82**, 323–355.
5. M. P. Mayer, Gymnastics of Molecular Chaperones, *Mol. Cell*, 2010, **39**, 321–331.
6. M. J. Avellaneda, E. J. Koers, M. M. Naqvi and S. J. Tans, The chaperone toolbox at the single-molecule level: From clamping to confining, *Protein Sci.*, 2017, **26**, 1291–1302.

7. A. Mashaghi, G. Kramer, D. C. Lamb, M. P. Mayer and S. J. Tans, Chaperone action at the single-molecule level, *Chem. Rev.*, 2014, **114**, 660–676.
8. S. Hiller, Chaperone-Bound Clients: The Importance of Being Dynamic, *Trends Biochem. Sci.*, 2019, **44**, 517–527.
9. G. J. Haran, How, when and why proteins collapse: the relation to folding, *Curr. Opin. Struct. Biol.*, 2012, **22**, 14–20.
10. M. Thommen, W. Holtkamp and M. V. Rodnina, Co-translational protein folding: progress and methods, *Curr. Opin. Struct. Biol.*, 2016, **42**, 83–89.
11. M. Taipale, D. F. Jarosz and S. Lindquist, HSP90 at the hub of protein homeostasis: emerging mechanistic insights, *Nat. Rev. Mol. Cell Biol.*, 2010, **11**, 515–528.
12. J. N. Wells, L. T. Bergendahl and J. A. Marsh, Co-translational assembly of protein complexes, *Biochem. Soc. Trans.*, 2015, **43**, 1221–1226.
13. K. Liberek, A. Lewandowska and S. Ziętkiewicz, Chaperones in control of protein disaggregation, *EMBO J.*, 2008, **27**, 328–335.
14. Y. Shin and C. P. Brangwynne, Liquid phase condensation in cell physiology and disease, *Science*, 2017, **357**, DOI: 10.1126/science.aaf4382.
15. R. Sousa, Structural mechanisms of chaperone mediated protein disaggregation, *Front. Mol. Biosci.*, 2014, **1**, DOI: 10.3389/fmolb.2014.00012.
16. H. Meyer and C. C. Wehl, The VCP/p97 system at a glance: connecting cellular function to disease pathogenesis, *J. Cell Sci.*, 2014, **127**, 3877–3883.
17. R. Zahn, S. Perrett and A. R. Fersht, Conformational states bound by the molecular chaperones GroEL and SecB: A hidden unfolding (annealing) activity, *J. Mol. Biol.*, 1996, **261**, 43–61.
18. C. M. Dobson, Protein folding and misfolding, *Nature*, 2003, **426**, 884–890.
19. M. Mickler, M. Hessling, C. Ratzke, J. Buchner and T. Hugel, The large conformational changes of Hsp90 are only weakly coupled to ATP hydrolysis, *Nat. Struct. Mol. Biol.*, 2009, **16**, 281–286.
20. L. D. Cabrita, *et al.*, A structural ensemble of a ribosome-nascent chain complex during cotranslational protein folding, *Nat. Struct. Mol. Biol.*, 2016, **23**, 278–285.
21. D. H. Chen, *et al.*, Visualizing GroEL/ES in the act of encapsulating a folding protein, *Cell*, 2013, **153**, 1354–1365.
22. B. M. Burmann, *et al.*, Regulation of alpha-synuclein by chaperones in mammalian cells, *Nature*, 2020, **577**, 127–132.
23. Z. Lin and H. S. Rye, Expansion and compression of a protein folding intermediate by GroEL, *Mol. Cell*, 2004, **16**, 23–34.
24. F. Georgescauld, *et al.*, GroEL/ES Chaperonin Modulates the Mechanism and Accelerates the Rate of TIM-Barrel Domain Folding, *Cell*, 2014, **157**, 922–934.
25. C. J. Bustamante, Y. R. Chemla, S. Liu and M. D. Wang, Optical tweezers in single-molecule biophysics, *Nat. Rev. Methods Primers*, 2021, **1**, DOI: 10.1038/s43586-021-00021-6.

26. C. Cecconi, E. A. Shank, C. Bustamante and S. Marqusee, Direct observation of the three-state folding of a single protein molecule, *Science*, 2005, **309**, 2057–2060.
27. J. P. Junker, F. Ziegler and M. Rief, Ligand-dependent equilibrium fluctuations of single calmodulin molecules, *Science*, 2009, **323**, 633–637.
28. M. M. Naqvi, *et al.*, Single-molecule folding mechanisms of the apo- and Mg(2+)-bound states of human neuronal calcium sensor-1, *Biophys. J.*, 2015, **109**, 113–123.
29. J. Perales-Calvo, D. Giganti, G. Stirnemann and S. Garcia-Manyes, The force-dependent mechanism of DnaK-mediated mechanical folding, *Sci. Adv.*, 2018, **4**, eaaq0243.
30. A. Mashaghi, *et al.*, Alternative modes of client binding enable functional plasticity of Hsp70, *Nature*, 2016, **539**, 448–451.
31. A. Mashaghi, *et al.*, Reshaping of the conformational search of a protein by the chaperone trigger factor, *Nature*, 2013, **500**, 98–101.
32. S. Haldar, R. Tapia-Rojo, E. C. Eckels, J. Valle-Orero and J. M. Fernandez, Trigger factor chaperone acts as a mechanical foldase, *Nat. Commun.*, 2017, **8**, DOI: 10.1038/s41467-017-00771-6.
33. M. M. Naqvi, *et al.*, Protein chain collapse modulation and folding stimulation by GroEL–ES, *Sci. Adv.*, 2022, **8**, eabl6293.
34. M. J. Avellaneda, *et al.*, Processive extrusion of polypeptide loops by a Hsp100 disaggregase, *Nature*, 2020, **74**, DOI: 10.1038/s41586-020-2017-2.
35. A. Ashkin, Optical trapping and manipulation of neutral particles using lasers, *Proc. Natl. Acad. Sci. U. S. A.*, 1997, **94**, 4853–4860.
36. K. Svoboda and S. M. Block, Biological Applications of Optical Forces, *Annu. Rev. Biophys. Biomol. Struct.*, 1994, **23**, 247–285.
37. C. J. Bustamante, Y. R. Chemla, S. Liu and M. D. Wang, Optical tweezers in single-molecule biophysics, *Nat. Rev. Methods Primers*, 2021, **1**, 25.
38. A. Ashkin, J. M. Dziedzic, J. E. Bjorkholm and S. Chu, Observation of a single-beam gradient force optical trap for dielectric particles, *Opt. Lett.*, 1986, **11**, 288–290.
39. A. D. Mehta, M. Rief, J. A. Spudich, D. A. Smith and R. M. Simmons, Single-Molecule Biomechanics with Optical Methods, *Science*, 1999, **283**, 1689–1695.
40. M. Ozkan, M. Wang, C. Ozkan, R. Flynn and S. Esener, Optical Manipulation of Objects and Biological Cells in Microfluidic Devices, *Biomed. Microdevices*, 2003, **5**, 61–67.
41. J. R. Moffitt, Y. R. Chemla, S. B. Smith and C. Bustamante, Recent advances in optical tweezers, *Annu. Rev. Biochem.*, 2008, **77**, 205–228.
42. C. Bustamante, Y. R. Chemla, N. R. Forde and D. Izhaky, Mechanical processes in biochemistry, *Annu. Rev. Biochem.*, 2004, **73**, 705–748.
43. D. Gao, *et al.*, Optical manipulation from the microscale to the nanoscale: fundamentals, advances and prospects, *Light: Sci. Appl.*, 2017, **6**, e17039.



44. M. J. Avellaneda, *et al.*, Processive extrusion of polypeptide loops by a Hsp100 disaggregase, *Nature*, 2020, **578**, 317–320.
45. I. Heller, *et al.*, STED nanoscopy combined with optical tweezers reveals protein dynamics on densely covered DNA, *Nat. Methods*, 2013, **10**, 910–916.
46. R. Kassies, *et al.*, Combined AFM and confocal fluorescence microscope for applications in bio-nanotechnology, *J. Microsc.*, 2005, **217**, 109–116.
47. F. E. Kemmerich, *et al.*, Simultaneous Single-Molecule Force and Fluorescence Sampling of DNA Nanostructure Conformations Using Magnetic Tweezers, *Nano Lett.*, 2016, **16**, 381–386.
48. C. Bustamante, Y. R. Chemla and J. R. Moffitt, High-resolution dual-trap optical tweezers with differential detection: instrument design, *Cold Spring Harb. Protoc.*, 2009, **2009**, pdb.ip73.
49. E. Rhoades, E. Gussakovsky and G. Haran, Watching proteins fold one molecule at a time, *Proc. Natl. Acad. Sci. U. S. A.*, 2003, **100**, 3197–3202.
50. B. Schuler and W. A. Eaton, Protein folding studied by single-molecule FRET, *Curr. Opin. Struct. Biol.*, 2008, **18**, 16–26.
51. A. N. Kapanidis and T. Strick, Biology, one molecule at a time, *Trends Biochem. Sci.*, 2009, **34**, 234–243.
52. P. O. Heidarsson, *et al.*, Direct single-molecule observation of calcium-dependent misfolding in human neuronal calcium sensor-1, *Proc. Natl. Acad. Sci. U. S. A.*, 2014, **111**, 13069–13074.
53. H. Yu, *et al.*, Direct observation of multiple misfolding pathways in a single prion protein molecule, *Proc. Natl. Acad. Sci. U. S. A.*, 2012, **109**, 5283–5288.
54. A. Mashaghi, S. Mashaghi and S. J. Tans, Misfolding of Luciferase at the Single-Molecule Level, *Angew. Chem.*, DOI: 10.1002/anie.2014055662014.
55. K. Svoboda, C. F. Schmidt, B. J. Schnapp and S. M. Block, Direct observation of kinesin stepping by optical trapping interferometry, *Nature*, 1993, **365**, 721–727.
56. C. L. Asbury, A. N. Fehr and S. M. Block, Kinesin moves by an asymmetric hand-over-hand mechanism, *Science*, 2003, **302**, 2130–2134.
57. J. W. Shaevitz, E. A. Abbondanzieri, R. Landick and S. M. Block, Backtracking by single RNA polymerase molecules observed at near-base-pair resolution, *Nature*, 2003, **426**, 684–687.
58. E. A. Abbondanzieri, W. J. Greenleaf, J. W. Shaevitz, R. Landick and S. M. Block, Direct observation of base-pair stepping by RNA polymerase, *Nature*, 2005, **438**, 460–465.
59. W. Grange, *et al.*, VirE2: a unique ssDNA-compacting molecular machine, *PLoS Biol.*, 2008, **6**, e44.
60. J. Liphardt, B. Onoa, S. B. Smith, I. J. Tinoco and C. Bustamante, Reversible unfolding of single RNA molecules by mechanical force, *Science*, 2001, **292**, 733–737.
61. C. Bustamante, L. Alexander, K. Maciuba and C. M. Kaiser, Single-Molecule Studies of Protein Folding with Optical Tweezers, *Annu. Rev. Biochem.*, 2020, **89**, 443–470.

62. S. Uemura, *et al.*, Peptide bond formation destabilizes Shine-Dalgarno interaction on the ribosome, *Nature*, 2007, **446**, 454–457.
63. J. D. Wen, *et al.*, Following translation by single ribosomes one codon at a time, *Nature*, 2008, **452**, 598–603.
64. D. H. Goldman, *et al.*, Ribosome. Mechanical force releases nascent chain-mediated ribosome arrest in vitro and in vivo, *Science*, 2015, **348**, 457–460.
65. A. Mashaghi, *et al.*, Alternative modes of client binding enable functional plasticity of Hsp70, *Nature*, 2016, 1–16.
66. W. J. Greenleaf, M. T. Woodside and S. M. Block, High-resolution, single-molecule measurements of biomolecular motion, *Annu. Rev. Biophys. Biomol. Struct.*, 2007, **36**, 171–190.
67. M. J. Avellaneda, E. J. Koers, D. P. Minde, V. Sunderlikova and S. J. Tans, Simultaneous sensing and imaging of individual biomolecular complexes enabled by modular DNA–protein coupling, *Commun. Chem.*, 2020, **3**, 20.
68. Y. Hao, C. Canavan, S. S. Taylor and R. A. Maillard, Integrated Method to Attach DNA Handles and Functionally Select Proteins to Study Folding and Protein-Ligand Interactions with Optical Tweezers, *Sci. Rep.*, 2017, **7**, 10843.
69. F. Moayed, A. Mashaghi and S. J. Tans, A polypeptide-DNA hybrid with selective linking capability applied to single molecule nano-mechanical measurements using optical tweezers, *PLoS One*, 2013, **8**, e54440.
70. C. Cecconi, E. A. Shank, F. W. Dahlquist, S. Marqusee and C. Bustamante, Protein-DNA chimeras for single molecule mechanical folding studies with the optical tweezers, *Eur. Biophys. J.*, 2008, **37**, 729–738.
71. M. Jahn, J. Buchner, T. Hugel and M. Rief, Folding and assembly of the large molecular machine Hsp90 studied in single-molecule experiments, *Proc. Natl. Acad. Sci. U. S. A.*, 2016, **113**, 1232–1237.
72. Z. Ganim and M. Rief, Mechanically switching single-molecule fluorescence of GFP by unfolding and refolding, *Proc. Natl. Acad. Sci. U. S. A.*, 2017, 201704937.
73. F. Wruck, A. Katranidis, K. H. Nierhaus, G. Büldt and M. Hegner, Translation and folding of single proteins in real time, *Proc. Natl. Acad. Sci. U. S. A.*, 2017, **114**, E4399–E4407.
74. C. M. Kaiser, D. H. Goldman, J. D. Chodera, I. Tinoco Jr. and C. Bustamante, The ribosome modulates nascent protein folding, *Science*, 2011, **334**, 1723–1727.
75. T. Liu, *et al.*, Direct measurement of the mechanical work during translocation by the ribosome, *eLife*, 2014, **3**, e03406.
76. W. Holtkamp, *et al.*, Cotranslational protein folding on the ribosome monitored in real time, *Science*, 2015, **350**, 1104–1107.
77. S. Bhushan, *et al.*,  $\alpha$ -Helical nascent polypeptide chains visualized within distinct regions of the ribosomal exit tunnel, *Nat. Struct. Mol. Biol.*, 2010, **17**, 313–317.

78. O. B. Nilsson, *et al.*, Cotranslational Protein Folding inside the Ribosome Exit Tunnel, *Cell Rep.*, 2015, **12**, 1533–1540.
79. F. Wruck, *et al.*, The ribosome modulates folding inside the ribosomal exit tunnel, *Commun. Biol.*, 2021, **4**, 523.
80. J. Lu and C. Deutsch, Electrostatics in the ribosomal tunnel modulate chain elongation rates, *J. Mol. Biol.*, 2008, **384**, 73–86.
81. C. A. Charneski and L. D. Hurst, Positively charged residues are the major determinants of ribosomal velocity, *PLoS Biol.*, 2013, **11**, e1001508.
82. P. Huter, *et al.*, Structural Basis for Polyproline-Mediated Ribosome Stalling and Rescue by the Translation Elongation Factor EF-P, *Mol. Cell*, 2017, **68**, 515–527.e516.
83. T. E. Quax, N. J. Claassens, D. Soll and J. van der Oost, Codon Bias as a Means to Fine-Tune Gene Expression, *Mol. Cell*, 2015, **59**, 149–161.
84. Y. Mao, H. Liu, Y. Liu and S. Tao, Deciphering the rules by which dynamics of mRNA secondary structure affect translation efficiency in *Saccharomyces cerevisiae*, *Nucleic Acids Res.*, 2014, **42**, 4813–4822.
85. B. Fritch, *et al.*, Origins of the Mechanochemical Coupling of Peptide Bond Formation to Protein Synthesis, *J. Am. Chem. Soc.*, 2018, **140**, 5077–5087.
86. S. E. Leininger, F. Trovato, D. A. Nissley and E. P. O'Brien, Domain topology, stability, and translation speed determine mechanical force generation on the ribosome, *Proc. Natl. Acad. Sci. U. S. A.*, 2019, **116**, 5523–5532.
87. K. C. Stein and J. Frydman, The stop-and-go traffic regulating protein biogenesis: How translation kinetics controls proteostasis, *J. Biol. Chem.*, 2019, **294**, 2076–2084.
88. A. Hoffmann, B. Bukau and G. Kramer, Structure and function of the molecular chaperone Trigger Factor, *Biochim. Biophys. Acta*, 2010, **1803**, 650–661.
89. F. Merz, *et al.*, Molecular mechanism and structure of Trigger Factor bound to the translating ribosome, *EMBO J.*, 2008, **27**, 1622–1632.
90. E. Crooke and W. Wickner, Trigger factor: a soluble protein that folds pro-OmpA into a membrane-assembly-competent form, *Proc. Natl. Acad. Sci. U. S. A.*, 1987, **84**, 5216–5220.
91. D. Baram, *et al.*, Structure of trigger factor binding domain in biologically homologous complex with eubacterial ribosome reveals its chaperone action, *Proc. Natl. Acad. Sci. U. S. A.*, 2005, **102**, 12017–12022.
92. C. M. Kaiser, *et al.*, Real-time observation of trigger factor function on translating ribosomes, *Nature*, 2006, **444**, 455–460.
93. L. Ferbitz, *et al.*, Trigger factor in complex with the ribosome forms a molecular cradle for nascent proteins, *Nature*, 2004, **431**, 590–596.
94. F. Wruck, *et al.*, Protein Folding Mediated by Trigger Factor and Hsp70: New Insights from Single-Molecule Approaches, *J. Mol. Biol.*, 2018, **430**, 438–449.

95. K. Liu, K. Maciuba and C. M. Kaiser, The Ribosome Cooperates with a Chaperone to Guide Multi-domain Protein Folding, *Mol. Cell*, 2019, **74**, 310–319.e317.
96. T. Saio, X. Guan, P. Rossi, A. Economou and C. G. Kalodimos, Structural basis for protein antiaggregation activity of the trigger factor chaperone, *Science*, 2014, **344**, 1250494.
97. A. Raine, M. Lovmar, J. Wikberg and M. Ehrenberg, Trigger factor binding to ribosomes with nascent peptide chains of varying lengths and sequences, *J. Biol. Chem.*, 2006, **281**, 28033–28038.
98. S. Haldar, R. Tapia-Rojo, E. C. Eckels, J. Valle-Orero and J. M. Fernandez, Trigger factor chaperone acts as a mechanical foldase, *Nat. Commun.*, 2017, **8**, 668.
99. D. Fan, *et al.*, Exploring the roles of substrate-binding surface of the chaperone site in the chaperone activity of trigger factor, *FASEB J.*, 2018, fj201701576.
100. K. Singhal, J. Vreede, A. Mashaghi, S. J. Tans and P. G. Bolhuis, The Trigger Factor Chaperone Encapsulates and Stabilizes Partial Folds of Substrate Proteins, *PLoS Comput. Biol.*, 2015, **11**, e1004444.
101. R. Maier, B. Eckert, C. Scholz, H. Lilie and F. X. Schmid, Interaction of trigger factor with the ribosome, *J. Mol. Biol.*, 2003, **326**, 585–592.
102. H. Patzelt, *et al.*, Three-state equilibrium of Escherichia coli trigger factor, *Biol. Chem.*, 2002, **383**, 1611–1619.
103. L. Morgado, B. M. Burmann, T. Sharpe, A. Mazur and S. Hiller, The dynamic dimer structure of the chaperone Trigger Factor, *Nat. Commun.*, 2017, **8**, 1992.
104. S. K. Lakshminpathy, *et al.*, Identification of nascent chain interaction sites on trigger factor, *J. Biol. Chem.*, 2007, **282**, 12186–12193.
105. A. Rutkowska, *et al.*, Dynamics of trigger factor interaction with translating ribosomes, *J. Biol. Chem.*, 2008, **283**, 4124–4132.
106. M. J. Avellaneda, E. J. Koers, D. P. Minde, V. Sunderlikova and S. J. Tans, Simultaneous sensing and imaging of individual biomolecular complexes enabled by modular DNA–protein coupling, *Commun. Chem.*, 2020, **3**, 20.
107. R. Rosenzweig, N. B. Nillegoda, M. P. Mayer and B. Bukau, The Hsp70 chaperone network, *Nat. Rev. Mol. Cell Biol.*, 2019, **20**, 665–680.
108. G. Calloni, *et al.*, DnaK functions as a central hub in the E. coli chaperone network, *Cell Rep.*, 2012, **1**, 251–264.
109. M. P. Mayer and B. Bukau, Hsp70 chaperones: cellular functions and molecular mechanism, *Cell. Mol. Life Sci.*, 2005, **62**, 670–684.
110. H. H. Kampinga and E. A. Craig, The HSP70 chaperone machinery: J proteins as drivers of functional specificity, *Nat. Rev. Mol. Cell Biol.*, 2010, **11**, 579–592.
111. M. E. Murphy, The HSP70 family and cancer, *Carcinogenesis*, 2013, **34**, 1181–1188.

112. R. Kityk, J. Kopp, I. Sinning and M. P. Mayer, Structure and dynamics of the ATP-bound open conformation of Hsp70 chaperones, *Mol. Cell*, 2012, **48**, 863–874.
113. M. Sikor, K. Mapa, L. V. von Voithenberg, D. Mokranjac and D. C. Lamb, Real-time observation of the conformational dynamics of mitochondrial Hsp70 by spFRET, *EMBO J.*, 2013, **32**, 1639–1649.
114. J. M. Nunes, M. Mayer-Hartl, F. U. Hartl and D. J. Muller, Action of the Hsp70 chaperone system observed with single proteins, *Nat. Commun.*, 2015, **6**, 6307.
115. R. Kellner, *et al.*, Single-molecule spectroscopy reveals chaperone-mediated expansion of substrate protein, *Proc. Natl. Acad. Sci. U. S. A.*, 2014, **111**, 13355–13360.
116. M. P. Mayer, *et al.*, Multistep mechanism of substrate binding determines chaperone activity of Hsp70, *Nat. Struct. Biol.*, 2000, **7**, 586–593.
117. J. Gamer, *et al.*, A cycle of binding and release of the DnaK, DnaJ and GrpE chaperones regulates activity of the Escherichia coli heat shock transcription factor sigma32, *EMBO J.*, 1996, **15**, 607–617.
118. A. S. Wentink, *et al.*, Molecular dissection of amyloid disaggregation by human HSP70, *Nature*, 2020, **587**, 483–488.
119. P. De Los Rios, A. Ben-Zvi, O. Slutsky, A. Azem and P. Goloubinoff, Hsp70 chaperones accelerate protein translocation and the unfolding of stable protein aggregates by entropic pulling, *Proc. Natl. Acad. Sci. U. S. A.*, 2006, **103**, 6166–6171.
120. A. L. Horwich, K. B. Low, W. A. Fenton, I. N. Hirshfield and K. Furtak, Folding in-Vivo of Bacterial Cytoplasmic Proteins - Role of GroEL, *Cell*, 1993, **74**, 909–917.
121. C. M. Dobson, Protein folding and misfolding, *Nature*, 2003, **426**, 884–890.
122. F. U. Hartl and M. Hayer-Hartl, Protein folding - Molecular chaperones in the cytosol: from nascent chain to folded protein, *Science*, 2002, **295**, 1852–1858.
123. A. L. Horwich and W. A. Fenton, Chaperonin-assisted protein folding: a chronologue, *Q. Rev. Biophys.*, 2020, **53**, e4.
124. H. R. Saibil, W. A. Fenton, D. K. Clare and A. L. Horwich, Structure and allostery of the chaperonin GroEL, *J. Mol. Biol.*, 2013, **425**, 1476–1487.
125. H. S. Rye, *et al.*, Distinct actions of cis and trans-ATP within the double ring of the chaperonin GroEL, *Nature*, 1997, **388**, 792–798.
126. P. B. Sigler, *et al.*, Structure and function in GroEL-mediated protein folding, *Annu. Rev. Biochem.*, 1998, **67**, 581–608.
127. H. S. Rye, *et al.*, GroEL–GroES cycling: ATP and nonnative polypeptide direct alternation of folding-active rings, *Cell*, 1999, **97**, 325–338.
128. M. Hayer-Hartl, A. Bracher and F. U. Hartl, The GroEL–GroES Chaperonin Machine: A Nano-Cage for Protein Folding, *Trends Biochem. Sci.*, 2016, **41**, 62–76.
129. A. L. Horwich, A. C. Apetri and W. A. Fenton, The GroEL/GroES cis cavity as a passive anti-aggregation device, *FEBS Lett.*, 2009, **583**, 2654–2662.

130. M. J. Todd, G. H. Lorimer and D. Thirumalai, Chaperonin-facilitated protein folding: optimization of rate and yield by an iterative annealing mechanism, *Proc. Natl. Acad. Sci. U. S. A.*, 1996, **93**, 4030–4035.
131. K. Chakraborty, *et al.*, Chaperonin-catalyzed rescue of kinetically trapped states in protein folding, *Cell*, 2010, **142**, 112–122.
132. M. M. Naqvi, *et al.*, Protein chain collapse modulation and folding stimulation by GroEL–ES, *Sci. Adv.*, 2022, **8**, eabl6293.
133. F. Motojima and M. Yoshida, Polypeptide in the chaperonin cage partly protrudes out and then folds inside or escapes outside, *EMBO J.*, 2010, **29**, 4008–4019.
134. C. Chaudhry, *et al.*, Role of the gamma-phosphate of ATP in triggering protein folding by GroEL–GroES: function, structure and energetics, *EMBO J.*, 2003, **22**, 4877–4887.
135. S. Priya, *et al.*, GroEL and CCT are catalytic unfoldases mediating out-of-cage polypeptide refolding without ATP, *Proc. Natl. Acad. Sci. U. S. A.*, 2013, **110**, 7199–7204.
136. S. Sharma, *et al.*, Monitoring protein conformation along the pathway of chaperonin-assisted folding, *Cell*, 2008, **133**, 142–153.
137. L. Hua, R. Zangi and B. J. Berne, Hydrophobic Interactions and Dewetting between Plates with Hydrophobic and Hydrophilic Domains, *J. Phys. Chem. C*, 2009, **113**, 5244–5253.
138. J. A. Riback, *et al.*, Innovative scattering analysis shows that hydrophobic disordered proteins are expanded in water, *Science*, 2017, **358**, 238–241.
139. J. L. England and V. S. Pande, Potential for modulation of the hydrophobic effect inside chaperonins, *Biophys. J.*, 2008, **95**, 3391–3399.
140. B. Schuler, A. Soranno, H. Hofmann and D. J. Nettels, Single-molecule FRET spectroscopy and the polymer physics of unfolded and intrinsically disordered proteins, *Annu. Rev. Biophys.*, 2016, **45**, 207–231.
141. J. Thoma, B. M. Burmann, S. Hiller and D. J. Muller, Impact of holdase chaperones Skp and SurA on the folding of beta-barrel outer-membrane proteins, *Nat. Struct. Mol. Biol.*, 2015, **22**, 795–802.
142. N. K. Tyagi, W. A. Fenton, A. A. Deniz and A. L. Horwich, Double mutant MBP refolds at same rate in free solution as inside the GroEL/GroES chaperonin chamber when aggregation in free solution is prevented, *FEBS Lett.*, 2011, **585**, 1969–1972.
143. A. J. Gupta, S. Haldar, G. Milicic, F. U. Hartl and M. Hayer-Hartl, Active cage mechanism of chaperonin-assisted protein folding demonstrated at single-molecule level, *J. Mol. Biol.*, 2014, **426**, 2739–2754.
144. J. Weaver, *et al.*, GroEL actively stimulates folding of the endogenous substrate protein PepQ, *Nat. Commun.*, 2017, **8**, 15934.
145. H. Hofmann, *et al.*, Single-molecule spectroscopy of protein folding in a chaperonin cage, *Proc. Natl. Acad. Sci. U. S. A.*, 2010, **107**, 11793–11798.
146. Y. Takei, R. Iizuka, T. Ueno and T. Funatsu, Single-molecule observation of protein folding in symmetric GroEL-(GroES)<sub>2</sub> complexes, *J. Biol. Chem.*, 2012, **287**, 41118–41125.

147. X. Ye and G. H. Lorimer, Substrate protein switches GroE chaperonins from asymmetric to symmetric cycling by catalyzing nucleotide exchange, *Proc. Natl. Acad. Sci. U. S. A.*, 2013, **110**, E4289–E4297.
148. S. Haldar, *et al.*, Chaperonin-Assisted Protein Folding: Relative Population of Asymmetric and Symmetric GroEL:GroES Complexes, *J. Mol. Biol.*, 2015, **427**, 2244–2255.
149. D. Noshiro and T. Ando, Substrate protein dependence of GroEL–GroES interaction cycle revealed by high-speed atomic force microscopy imaging, *Philos. Trans. R. Soc. London, Ser. B*, 2018, **373**, 20170180.
150. E. Kirschke, D. Goswami, D. Southworth, P. R. Griffin and D. A. Agard, Glucocorticoid receptor function regulated by coordinated action of the Hsp90 and Hsp70 chaperone cycles, *Cell*, 2014, **157**, 1685–1697.
151. T. Moran Luengo, R. Kityk, M. P. Mayer and S. G. D. Rudiger, Hsp90 Breaks the Deadlock of the Hsp70 Chaperone System, *Mol. Cell*, 2018, **70**, 545–552.e549.
152. M. Taipale, *et al.*, Quantitative analysis of HSP90-client interactions reveals principles of substrate recognition, *Cell*, 2012, **150**, 987–1001.
153. G. I. Karras, *et al.*, HSP90 Shapes the Consequences of Human Genetic Variation, *Cell*, 2017, **168**, 856–866.e812.
154. L. Whitesell and S. L. Lindquist, HSP90 and the chaperoning of cancer, *Nat. Rev. Cancer*, 2005, **5**, 761–772.
155. X. Yan and L. Yajun, Recent Advances in the Discovery of Novel HSP90 Inhibitors: An Update from 2014, *Curr. Drug Targets*, 2020, **21**, 302–317.
156. M. Jahn, J. Buchner, T. Hugel and M. Rief, Folding and assembly of the large molecular machine Hsp90 studied in single-molecule experiments, *Proc. Natl. Acad. Sci. U. S. A.*, 2016, **113**, 1232–1237.
157. M. Jahn, *et al.*, Folding and Domain Interactions of Three Orthologs of Hsp90 Studied by Single-Molecule Force Spectroscopy, *Structure*, 2018, **26**, 96–105.e104.
158. G. E. Karagöz, *et al.*, Hsp90-Tau complex reveals molecular basis for specificity in chaperone action, *Cell*, 2014, **156**, 963–974.
159. K. A. Verba, *et al.*, Atomic structure of Hsp90-Cdc37-Cdk4 reveals that Hsp90 traps and stabilizes an unfolded kinase, *Science*, 2016, **352**, 1542–1547.
160. C. M. Noddings, R. Y.-R. Wang, J. L. Johnson and D. A. Agard, Structure of Hsp90–p23–GR reveals the Hsp90 client-remodelling mechanism, *Nature*, 2021, **601**, 465–469.
161. R. Y.-R. Wang, *et al.*, GR chaperone cycle mechanism revealed by cryo-EM: inactivation of GR by GR:Hsp90:Hsp70:Hsp client-loading complex, *bioRxiv*, 2020, preprint, DOI: 10.1101/2020.11.05.370247.
162. A. Mashaghi, *et al.*, Direct observation of Hsp90-induced compaction in a protein chain, *Cell Rep.*, 2022, **41**, DOI: 10.1016/j.celrep.2022.111734.
163. K. A. Dill, Theory for the folding and stability of globular proteins, *Biochemistry*, 1985, **24**, 1501–1509.

164. P. O. Heidarsson, *et al.*, A highly compliant protein native state with a spontaneous-like mechanical unfolding pathway, *J. Am. Chem. Soc.*, 2012, **134**, 17068–17075.
165. P. S. Kim and R. L. Baldwin, Specific intermediates in the folding reactions of small proteins and the mechanism of protein folding, *Annu. Rev. Biochem.*, 1982, **51**, 459–489.
166. T. R. Alderson, *et al.*, Local unfolding of the HSP27 monomer regulates chaperone activity, *Nat. Commun.*, 2019, **10**, 1068.
167. E. Basha, H. O'Neill and E. Vierling, Small heat shock proteins and alpha-crystallins: dynamic proteins with flexible functions, *Trends Biochem. Sci.*, 2012, **37**, 106–117.
168. C. L. Johnston, *et al.*, Single-molecule fluorescence-based approach reveals novel mechanistic insights into human small heat shock protein chaperone function, *J. Biol. Chem.*, 2021, **296**, 100161.
169. S. Ungelenk, *et al.*, Small heat shock proteins sequester misfolding proteins in near-native conformation for cellular protection and efficient refolding, *Nat. Commun.*, 2016, **7**, 13673.
170. A. G. Cashikar, M. Duennwald and S. L. Lindquist, A chaperone pathway in protein disaggregation. Hsp26 alters the nature of protein aggregates to facilitate reactivation by Hsp104, *J. Biol. Chem.*, 2005, **280**, 23869–23875.
171. A. Mogk, E. Deuerling, S. Vorderwulbecke, E. Vierling and B. Bukau, Small heat shock proteins, ClpB and the DnaK system form a functional triade in reversing protein aggregation, *Mol. Microbiol.*, 2003, **50**, 585–595.
172. F. Moayed, *et al.*, The Anti-Aggregation Holdase Hsp33 Promotes the Formation of Folded Protein Structures, *Biophys. J.*, 2020, **118**, 85–95.
173. D. Reichmann, *et al.*, Order out of disorder: working cycle of an intrinsically unfolded chaperone, *Cell*, 2012, **148**, 947–957.
174. A. Mogk, C. Ruger-Herreros and B. Bukau, Cellular Functions and Mechanisms of Action of Small Heat Shock Proteins, *Annu. Rev. Microbiol.*, 2019, **73**, 89–110.
175. A. Mogk, E. Kummer and B. Bukau, Cooperation of Hsp70 and Hsp100 chaperone machines in protein disaggregation, *Front. Mol. Biosci.*, 2015, **2**, 22.
176. O. Faust, *et al.*, HSP40 proteins use class-specific regulation to drive HSP70 functional diversity, *Nature*, 2020, **587**, 489–494.
177. J. Tittelmeier, *et al.*, The HSP110/HSP70 disaggregation system generates spreading-competent toxic  $\alpha$ -synuclein species, *EMBO J.*, 2020, **39**, e103954.
178. N. B. Nillegoda, *et al.*, Crucial HSP70 co-chaperone complex unlocks metazoan protein disaggregation, *Nature*, 2015, **524**, 247–251.
179. S. M. Doyle and S. Wickner, Hsp104 and ClpB: protein disaggregating machines, *Trends Biochem. Sci.*, 2009, **34**, 40–48.
180. Y. Oguchi, *et al.*, A tightly regulated molecular toggle controls AAA+ disaggregase, *Nat. Struct. Mol. Biol.*, 2012, **19**, 1338–1346.



181. H. Mazal, *et al.*, Tunable microsecond dynamics of an allosteric switch regulate the activity of a AAA+ disaggregation machine, *Nat. Commun.*, 2019, **10**, 1–12.
182. M. E. Aubin-Tam, A. O. Olivares, R. T. Sauer, T. A. Baker and M. J. Lang, Single-molecule protein unfolding and translocation by an ATP-fueled proteolytic machine, *Cell*, 2011, **145**, 257–267.
183. R. A. Maillard, *et al.*, ClpX(P) generates mechanical force to unfold and translocate its protein substrates, *Cell*, 2011, **145**, 459–469.
184. A. O. Olivares, A. R. Nager, O. Iosefson, R. T. Sauer and T. A. Baker, Mechanochemical basis of protein degradation by a double-ring AAA+ machine, *Nat. Struct. Mol. Biol.*, 2014, **21**, 871–875.
185. C. L. Durie, *et al.*, Hsp104 and Potentiated Variants Can Operate as Distinct Nonprocessive Translocases, *Biophys. J.*, 2019, **116**, 1856–1872.
186. T. Li, *et al.*, Escherichia coli ClpB is a non-processive polypeptide translocase, *Biochem. J.*, 2015, **470**, 39–52.
187. S. N. Gates, *et al.*, Ratchet-like polypeptide translocation mechanism of the AAA+ disaggregase Hsp104, *Science*, 2017, **357**, 273–279.
188. T. Haslberger, *et al.*, Protein disaggregation by the AAA+ chaperone ClpB involves partial threading of looped polypeptide segments, *Nat. Struct. Mol. Biol.*, 2008, **15**, 641–650.
189. T. Uchihashi, *et al.*, Dynamic structural states of ClpB involved in its disaggregation function, *Nat. Commun.*, 20182021, **9**, 2147.
190. J. van den Boom, *et al.*, Targeted substrate loop insertion by VCP/p97 during PP1 complex disassembly, *Nat. Struct. Mol. Biol.*, 1–8.
191. H. Han, *et al.*, Structure of Vps4 with circular peptides and implications for translocation of two polypeptide chains by AAA+ ATPases, *eLife*, 2019, **8**, e44071.
192. C. Deville, K. Franke, A. Mogk, B. Bukau and H. R. Saibil, Two-step activation mechanism of the ClpB disaggregase for sequential substrate threading by the main ATPase motor, *Cell Rep.*, 2019, **27**, 3433–3446.e3434.
193. H. Mazal, M. Iljina, I. Riven and G. Haran, Ultrafast pore-loop dynamics in a AAA+ machine point to a Brownian-ratchet mechanism for protein translocation, *Sci. Adv.*, 2021, **7**, eabg4674.
194. A. N. Rizo, *et al.*, Structural basis for substrate gripping and translocation by the ClpB AAA+ disaggregase, *Nat. Commun.*, 2019, **10**, 1–12.
195. K. L. Zuromski, R. T. Sauer and T. A. Baker, Modular and coordinated activity of AAA+ active sites in the double-ring ClpA unfoldase of the ClpAP protease, *Proc. Natl. Acad. Sci. U. S. A.*, 2020, **117**, 25455–25463.
196. O. Iosefson, A. O. Olivares, T. A. Baker and R. T. Sauer, Dissection of axial-pore loop function during unfolding and translocation by a AAA+ proteolytic machine, *Cell Rep.*, 2015, **12**, 1032–1041.
197. P. Rodriguez-Aliaga, L. Ramirez, F. Kim, C. Bustamante and A. Martin, Substrate-translocating loops regulate mechanochemical coupling and power production in AAA+ protease ClpXP, *Nat. Struct. Mol. Biol.*, 2016, **23**, 974–981.

198. J. Shorter and S. Lindquist, Hsp104 catalyzes formation and elimination of self-replicating Sup35 prion conformers, *Science*, 2004, **304**, 1793–1797.
199. D. M. Johnston, M. Miot, J. R. Hoskins, S. Wickner and S. M. Doyle, Substrate discrimination by ClpB and Hsp104, *Front. Mol. Biosci.*, 2017, **4**, 36.
200. K. Neupane, A. Solanki, I. Sosova, M. Belov and M. T. Woodside, Diverse metastable structures formed by small oligomers of  $\alpha$ -synuclein probed by force spectroscopy, *PLoS One*, 2014, **9**, e86495.
201. H. Yu, *et al.*, Direct observation of multiple misfolding pathways in a single prion protein molecule, *Proc. Natl. Acad. Sci. U. S. A.*, 2012, **109**, 5283–5288.
202. S. Vashist, M. Cushman and J. Shorter, Applying Hsp104 to protein-misfolding disorders, *Biochem. Cell Biol.*, 2010, **88**, 1–13.
203. P. Bechtluft, *et al.*, Direct observation of chaperone-induced changes in a protein folding pathway, *Science*, 2007, **318**, 1458–1461.
204. K. Singhal, J. Vreede, A. Mashaghi, S. J. Tans and P. G. Bolhuis, The Trigger Factor Chaperone Encapsulates and Stabilizes Partial Folds of Substrate Proteins, *PLoS Comput. Biol.*, 2015, **11**, e1004444.
205. L. P. Bergeron-Sandoval, N. Safaee and S. W. Michnick, Mechanisms and Consequences of Macromolecular Phase Separation, *Cell*, 2016, **165**, 1067–1079.
206. G. Kramer, D. Boehringer, N. Ban and B. Bukau, The ribosome as a platform for co-translational processing, folding and targeting of newly synthesized proteins, *Nat. Struct. Mol. Biol.*, 2009, **16**, 589–597.
207. Y. W. Shieh, *et al.*, Operon structure and cotranslational subunit association direct protein assembly in bacteria, *Science*, 2015, **350**, 678–680.
208. M. Bertolini, *et al.*, Interactions between nascent proteins translated by adjacent ribosomes drive homomer assembly, *Science*, 2021, **371**, 57–64.
209. T. O. Street, L. A. Lavery and D. A. Agard, Substrate binding drives large-scale conformational changes in the Hsp90 molecular chaperone, *Mol. Cell*, 2011, **42**, 96–105.